The effect of excessive medio-lateral trunk movements on ankle plantar flexor work during gait in healthy individuals

Bente Bloks

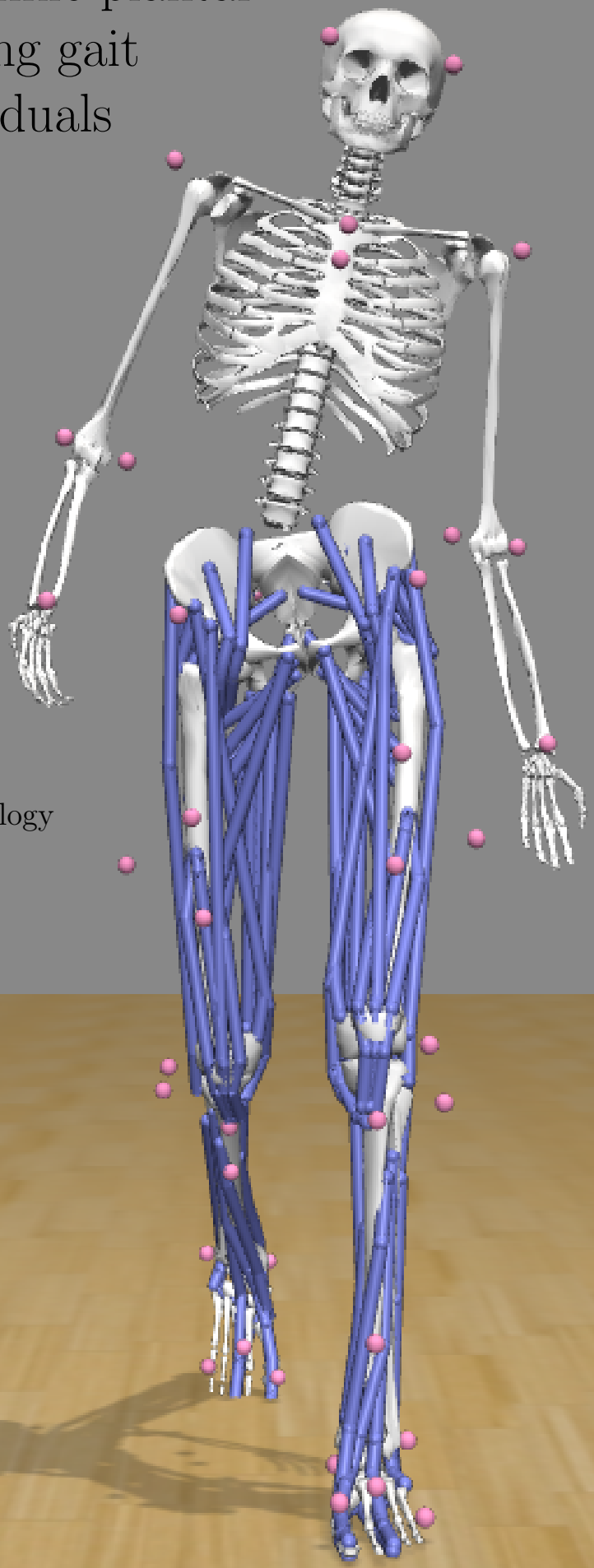

Master thesis

Delft University of Technology

November 2020

The effect of excessive medio-lateral trunk movements on ankle plantar flexor work during gait in healthy individuals

Bente Bloks

Student number: 4749901
27 November 2020

Thesis in partial fulfillment of the requirements for the degree of Master of Science in

Biomedical Engineering

at Delft University of Technology,

Master thesis project (BM51032)
Dept. of Biomechanical Engineering,
TU Delft
March 2020 - November 2020

Supervisors:
dr. ir. A. Seth
Prof. dr. ir. J. Harlaar

Thesis committee:
Prof. dr. ir. M. Wisse

Contents

List of Figures

List of Tables

Abstract

The ankle plantar flexion muscles are the main contributors to the propulsion of the body during gait. Deficits in these muscles, such as reduced muscle strength, often lead to impaired walking. A characteristic widely observed in gaits arising from various pathologies is an increase in medio-lateral trunk movements. However, this is not yet identified as a compensation strategy for ankle plantar flexor weakness. A previous analysis showed a decrease in positive work generated at the ankle joint in healthy individuals walking with excessive trunk sway compared to normal walking at the same speed. This suggests that excessive trunk sway could be used to compensate for a reduction in propulsive power generated at the ankle joint. This study investigates the relationship between excessive trunk movements in the frontal plane and propulsive power generated at the ankle joint by examining the contributions of individuals muscles to the total power generation during gait. The first aim of this study is to evaluate the validity of the previous results. The second aim is to uncover the underlying biomechanical compensatory mechanisms of walking with excessive medio-lateral trunk movements.

A data set consisting of marker data and ground reaction force data of healthy individuals walking with and without excessive medio-lateral trunk movements is analysed in this study. Three-dimensional muscle-actuated simulations of the recorded gaits were generated in OpenSim. A residual reduction algorithm was applied to make the kinematic outcomes more dynamically consistent with the experimentally measured ground reaction forces and moments. This is in contrast to the previous analysis, in which the residuals were not reduced. The power and work generated by the total system and the individual segments, joints and muscles were derived from the simulations.

An increase in positive work at the lumbar joint was found, but no differences in positive work at the hip, knee and/ or ankle joints were found over the gait cycle. The lumbar bending muscles turned out to be responsible for the increase in positive work at the lumbar joint.

In conclusion, we did not find medio-lateral trunk sway to be a compensatory mechanism for ankle plantar flexor weakness. Therefore, more research is needed to understand why trunk sway is commonly observed in patients with reduced plantar flexion muscle strength. The results of our study contrast those of the previous analysis. Our findings suggest that the discrepancy between the outcomes is caused by high residual forces and moments in the previous analysis. Hence, by revealing the discrepancy between the results of this study and the results of the previous analysis, this study highlights the importance of the validation of results before drawing conclusions.

Chapter 1

Introduction

The ankle plantar flexion muscles play an important role in human walking. With approximately two thirds of the total positive work that is generated by the plantar flexion muscles, the plantar flexors are the main contributors to the propulsion of the body during gait [44]. The work that is generated by the plantar flexors is mainly generated during the push-off phase of walking. This phase is characterized by a rapid contraction of the calf muscles that causes redirection of the body centre of mass (CoM) and generates the energy that is required to move the limbs forward [17].

Since the plantar flexors have such an important role in human gait, deficits in these muscles, such as reduced muscle strength, often lead to impaired walking. Reduced plantar flexion muscle strength can be caused by disuse, aging and diseases such as Parkinson's disease, cerebral palsy and stroke [35], [8], [30], [15]. Patients that are suffering from plantar flexor weakness are often using compensation strategies to overcome the reduction in propulsive power. One of the compensation strategies that was found by several studies is the increase in hip power [16], [30], [24], [22], [42]. Lewis and Ferris studied the effect of an increased and decreased ankle push-off power on the lower limb joint powers [16]. Healthy subjects were instructed to push less and more than normal with their feet while walking. It was found that an increase in ankle push-off power was related to a decrease in hip power. However, no such relationship was found between ankle and hip power for the condition with less ankle push-off. The results of this study suggest that the interplay between hip and ankle power during gait can be used as a compensation strategy to overcome a reduction in propulsive power of one of these joints. In the study that was performed by Riad and colleagues a shift in power generation between the ankle and hip joints was found as well [30]. In this study joint powers in children with spastic hemiplegic cerebral palsy and age matched healthy subjects were compared. An increased hip power and a decreased ankle power were found in the cerebral palsy group. This indicates that children with spastic hemiplegic cerebral palsy compensate for plantar flexion muscle weakness by an increased hip power. This same shift in power generation from the ankle joints to the hip joints was found by Waterval and colleagues [42]. In this study patients with unilateral calf muscle weakness participated. Gait kinematics and ground reaction forces were measured for walking at a preferred walking speed and at a matched control speed. What was found is that the reduction in calf muscle strength was compensated by a reduction in preferred walking speed. When this was not possible, because subjects had to walk at a matched control speed, an increase

in positive joint work at the ipsilateral hip and/ or contralateral hip, knee and ankle joints was found. In conclusion, there seems to be an interplay between hip and ankle power for the generation of propulsive power during gait. This means, patients with reduced muscle strength of either the hip or ankle muscles can compensate for this by increasing the power generation at the other joint.

Besides an increase in hip power, patients with plantar flexor weakness often show typical adjustments in gait kinematics as well. For example, one of the characteristics of a walking pattern that is affected by cerebral palsy is an increase in medio-lateral trunk movements [1], [12]. However, this is not yet identified as a compensation strategy for ankle plantar flexor weakness [34], [6]. Yet, the excessive trunk sway that can be observed in patients with cerebral palsy is often associated with reduced hip abductor strength [34], [2], [6]. Patients compensate for the hip abductor weakness by moving their trunk and thereby their CoM laterally towards the stance leg, which decreases the hip abductor moment [34], [33]. Nevertheless, the cause of the excessive medio-lateral trunk movements in patients with cerebral palsy is not yet completely clear. Krautwurst and colleagues studied the relationship between hip abductor weakness and excessive trunk sway [13]. They found that there was only a weak, yet significant, relationship between excessive trunk sway and hip abductor strength. According to the authors, this indicates that hip abductor weakness influences the medio-lateral movements of the trunk during gait. However, since the correlation was only weak, other factors that influence medio-lateral trunk movements during gait seem to be involved as well. Rethwilm and colleagues also studied excessive trunk sway in patients with cerebral palsy [29]. The aim of this study was to identify underlying biomechanical compensatory mechanisms of the increase in trunk movements in patients with cerebral palsy. However, no clear compensation strategies were found in this study that could be related to the increase in trunk movements. In conclusion, although excessive medio-lateral trunk movements can be observed in patients with cerebral palsy and in multiple other pathological gaits, the underlying compensation strategy of excessive trunk sway is still partly unknown. The fact that excessive trunk sway is widely observed suggests that trunk sway is an important factor in pathological gaits and therefore it would be valuable to investigate the underlying compensatory mechanisms of excessive medio-lateral trunk movements.

This study investigates the effect of excessive trunk sway on the power flow during gait in healthy individuals. In this way, it is attempted to identify the underlying compensatory mechanisms of excessive medio-lateral trunk movements. A previous analysis already showed an increase in total positive joint work in healthy individuals walking with excessive trunk sway compared to normal walking at the same speed [39]. Interestingly, it was found that the amount of positive work increased during the first half of the stance phase and decreased during the push-off phase. This was attributed to an increase in positive hip work and a decrease in positive ankle work. Furthermore, the total positive work at the lumbosacral joint increased. The reduction in positive work generated at the ankle joint suggests that there is an interplay between medio-lateral trunk movements and power generation at the ankle joint. Excessive medio-lateral trunk movements could therefore be part of a compensation mechanism to overcome reduced propulsive power due to ankle plantar flexion muscle weakness.

To understand how excessive trunk movements in the frontal plane can contribute to a reduction in propulsive power generated at the ankle joint, the contributions of individual muscles to the total power generation are investigated in this study. Since healthy human gait is achieved by complex muscle activation patterns, differences in muscle activity between walking with and without excessive trunk sway could provide insight into the underlying biomechanical mechanisms of walking with excessive trunk sway. Healthy subjects are participating in this study, since this will make it possible to distinguish between primary deviations in muscle activation patterns caused by the underlying pathology and secondary deviations due to the biomechanics of walking with excessive trunk sway when comparing the results to observations of pathological gait [32]. These insights could contribute to the determination of appropriate treatment of patients with reduced calf muscle strength and could be valuable for the development of assistive devices such as an ankle-foot orthosis.

1.1 Research questions

A previous analysis showed a reduction in ankle push-off power and an increase in total positive joint power when walking with excessive medio-lateral trunk movements [39]. The first aim of this study is to evaluate the validity of the results obtained by this previous analysis. Residual forces and moments are non-physical compensatory forces and moments that account for dynamic inconsistencies between the joint accelerations estimated from the experimental markers and the ground reaction force data [4]. Since the residual forces and moments, representing the experimental and modelling errors, were not reduced in the previous analysis, it is hypothesized that reducing the residuals to make the kinematic outcomes more dynamically consistent with the experimentally measured ground reaction forces and moments could have a significant effect on the outcomes.

The second aim of this study is to uncover the underlying biomechanical compensatory mechanisms of walking with excessive medio-lateral trunk movements by examining individual muscle powers. The question that arises from the results of the previous analysis is how the excessive trunk movements in the frontal plane could lead to a reduction in ankle push-off power compared to walking without excessive trunk sway at the same speed. Since muscles, including multi-articular muscles, have a complex interaction with the dynamics of the body segments, it is hypothesized that muscles are responsible for the transfer of power between joints, segments and planes [45]. Therefore, the individual muscle contributions to the power generation are studied, since it is assumed that this could give insight into the underlying mechanism between medio-lateral trunk movements and ankle push-off power. This leads to the following research questions:

- *Are the results obtained by the previous analysis reproducible using a data processing method in which the residual forces and moments will be reduced?*
- *Can the relationship between excessive medio-lateral trunk movements and power generation at the ankle joint be explained by differences in individual muscle contributions to the total power generation during gait in healthy individuals walking with and without excessive trunk sway?*

Chapter 2

Methodology

2.1 Data

The data set that is analysed in this study consists of motion data that was collected at the BioMechaMotion Lab at the Delft University of Technology (TU Delft) [41]. Eleven healthy subjects walked down a walkway of approximately seven meters with in the middle of the walkway two Kistler force plates of type 92060AA (Kistler, Winterthur, Switzerland). Ground reaction forces were recorded at a sample frequency of 1000 Hz. Fifty-three passive markers were placed on the subject's feet, lower legs, upper legs, pelvis, trunk, upper arms, lower arms and head. The markers are depicted in figure 2.1 and an overview of all the markers can be found in appendix A. The markers were tracked by twelve Oqus 700 motion capture cameras at 100 Hz (Qualysis, Gothenburg, Sweden). Marker position data and force plate data were collected for two different walking conditions. In the first condition subjects were asked to walk at 80% of their preferred walking speed, whereas in the second condition subjects had the task to walk with excessive medio-lateral trunk movements. Three successful trials were collected for each subject for each condition. Since for one of the subjects the static trial failed, this subject was excluded. An overview of the subject characteristics can be found in appendix B.

2.2 Data analysis

2.2.1 OpenSim

Model

OpenSim was used to analyse the data. The model that was used in OpenSim is a full body model that has 19 joints and consists of 22 connected bodies (Fig. 2.2 - 2.3) [27]. The mtp, subtalar and wrist joints were locked during the analyses. The model includes 80 muscles and 17 linear actuators representing the upper body muscles. A list of all the muscles and linear actuators can be found in appendix C.

Scaling

The first step in the data analysis was to scale the model for each subject based on the subject characteristics [4]. This means, the dimensions of each body segment were

adjusted based on marker position data. Furthermore, the mass properties of the model were scaled based on the subject's mass and the muscle lengths were adjusted. The first step in the scaling process was to 'prescale' the unscaled model based on the length of the subject. Next, model marker positions were adjusted based on the errors between the model and experimental markers during the three normal walking trials. After that, the model was scaled a second time. This time, the bodies were scaled based on scaling factors that were specified for each body. The scaling factors were based on the positions of the markers that were placed on anatomical landmarks. This process of adjusting the model markers and scaling the subject was iterated several times until the errors between the model and experimental markers were low for the three normal walking trials (root mean square (RMS) errors around 1 cm). Thereafter, the pelvis markers were rotated with the mean pelvis tilt angle that was measured during the three normal walking trials. This was done, because excessive pelvis tilt angles were observed before rotating the pelvis markers. Since it was assumed that this was caused by an incorrect placement of the pelvis markers on the body of the subject, the pelvis markers on the model were adjusted to account for this. Finally, the length of the pelvis was scaled with a manual scale factor of 0.95, because it was observed that this led to a decrease in errors between the experimental and model markers and that the dimensions of the pelvis looked more natural in this way.

Based on the errors between the model and experimental markers, it was decided that the scaled model was good enough to continue the data analysis (mean total RMS errors for the normal and trunk sway conditions were 0.98 ± 0.13 cm and 1.19 ± 0.27 cm). Moreover, for one of the subjects, the model was also scaled solely based on the marker positions during the static trial, instead of the marker positions during the normal walking trials. The power flows for the two walking conditions were calculated using the two differently scaled models. No differences were found between the power outcomes of the two differently scaled models and therefore it was decided that the scaling results were good, since small differences in the way the model was scaled did not influence the results.

Inverse kinematics

The scaled models were used to perform the inverse kinematic (IK) analyses. To determine the joint angles and translations a least-squares problem was solved that minimizes the differences between the marker positions of the model and the experimentally measured marker positions [4].

Residual Reduction Algorithm

A Residual Reduction Algorithm (RRA) was applied to make the kinematic outcomes more dynamically consistent with the experimentally measured ground reaction forces and moments [4]. This was done by applying small adjustments to the motion trajectory and to the mass characteristics of the model which leads to a reduction of the residual forces and moments. The RRA was only applied for the time interval for which complete force data was available. Since only two force plates were used in this study, it was not possible to analyse a complete gait cycle. It was tried

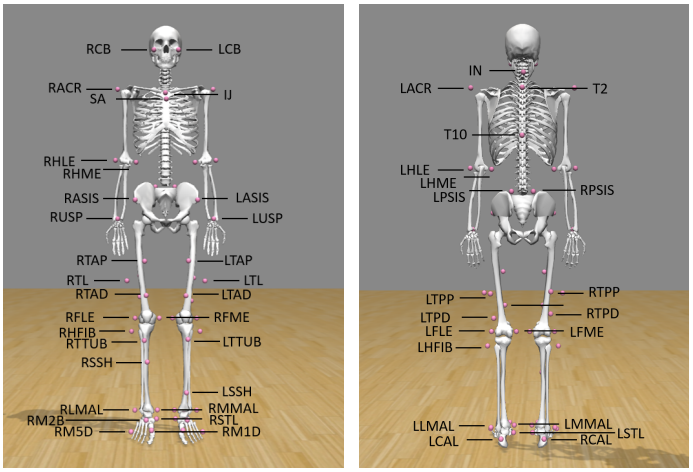

(a) Front (b) Back

Figure 2.1: Model markers. *An overview of all the markers is given in appendix A.*

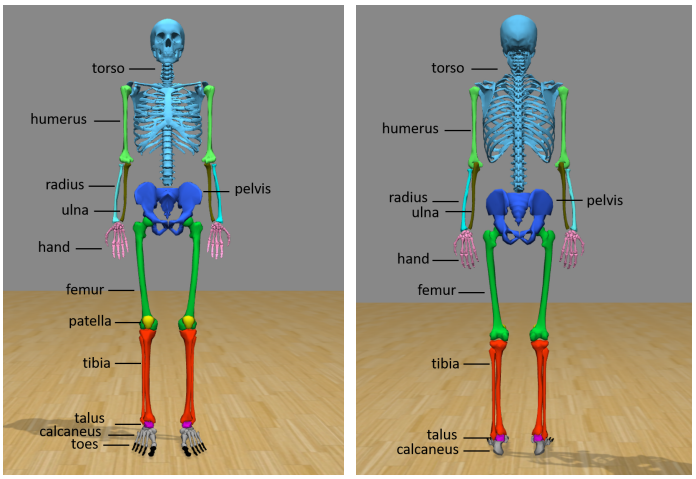

(a) Front (b) Back

Figure 2.2: Model bodies. *The model consists of 22 connected bodies which can be distinguished by the different colours in this figure.*

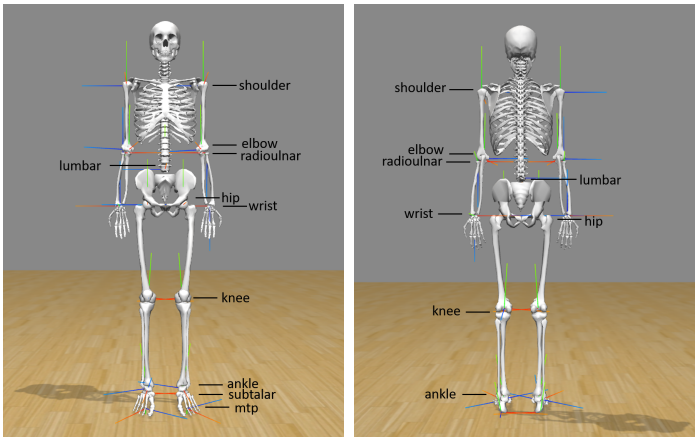

(a) Front (b) Back

Figure 2.3: Model joints. *The model consists of 13 free joints. The wrist, subtalar and mtp joints were locked during the analyses.*

to replicate the ground reaction forces and moments to simulate a third, virtual force plate. However, residual forces and moments increased excessively when these replicated ground reaction forces and moments were added. Therefore, it was concluded that there was too much variability in ground reaction force data to replicate the forces and moments. Hence, the analysis was done from the start of the midstance phase till the end of the gait cycle, defined by initial contact. More information about the definition of the gait phases will be provided in section 2.2.3.

To reduce the residual forces and moments, several iterations of the RRA were required. During the first iteration, the scaled model together with the IK solutions and the ground reaction forces and moments were used as inputs. Noise was removed from the ground reaction force data by putting all the ground reaction forces and moments to zero for the time intervals where the foot did not touch the force plate. Initial tracking weights for the coordinates were described in the 'RRA Tasks' file. Actuators for each degree of freedom were defined in the 'RRA Actuators' file. The settings were saved in the 'RRA Setup' file. After the first iteration, torso mass and torso CoM location were adjusted manually based on the suggested adjustments by OpenSim. It was chosen to adjust the torso CoM location manually, because the changes in CoM location performed by OpenSim were applied in the wrong direction, causing the residual moments to increase. A second RRA run was performed with the same tracking weights as during the first iteration, but with the adjusted model. The model mass and CoM location were not adjusted after this iteration. Kinematic errors were evaluated. A third and final RRA run was performed with the model that was adjusted after the first iteration. For this third iteration, tracking weights were decreased for coordinates for which the error was lower than one degree after the second iteration. The results were evaluated based on the contribution of the residuals to the total positive work that was generated.

Computed Muscle Control

Next, a Computed Muscle Control (CMC) algorithm was used to find a set of muscle excitations that produce a coordinated simulation of the walking pattern [4]. In this way, the contribution of each muscle to the generated power can be calculated and compared between the two walking conditions. The adjusted model that was created after applying the RRA was used in the CMC tool. The kinematic outcomes of the RRA and the ground reaction force data were also used as inputs for the CMC tool. The tracking weights, which were the same as used for the RRA tool, were described in the 'CMC Tasks' file. The actuators were described in the 'CMC Actuators' file and the control constraints were described in the 'CMC Control Constraints' file. The settings were saved in the 'CMC Setup' file.

2.2.2 Power and work calculations

The kinematic and kinetic outcomes of the RRA tool were used to calculate the external power [39]. The first step in calculating the external power is to calculate the individual limb CoM power. The individual limb CoM power can be calculated by taking the dot product of the external forces that are acting on both limbs and the velocity of the CoM (Eq. 2.1). The next step is to calculate the peripheral rate

of energy change. This can be done by calculating the changes in kinetic energy relative to the body's CoM, assuming 22 (N_s) rigid body segments (s) (Fig. 2.2) (Eq. 2.2). The external power can then be calculated by taking the sum of the individual limb CoM powers and the peripheral rate of energy change (Eq. 2.3).

$$P_{CoM} = \overrightarrow{\mathrm{F}} \cdot \overrightarrow{v}_{CoM} \tag{2.1}$$

$$\dot{E}_{per} = \frac{d}{dt}(\sum_{s}^{N_s} \frac{1}{2} \overrightarrow{I}_{seg} \overrightarrow{\omega}^2_{seg} + \frac{1}{2} m_{seg} (\overrightarrow{v}_{seg} - \overrightarrow{v}_{CoM})^2) \tag{2.2}$$

$$P_{tot} = P_{CoM} + \dot{E}_{per} \tag{2.3}$$

In equations 2.1-2.3, P_{CoM} is the individual limb CoM power, $\overrightarrow{\mathrm{F}}$ is the ground reaction force data, $\overrightarrow{v}_{CoM}$ is the linear velocity of the CoM of the total system and $\dot{E}_{per}$ is the peripheral rate of energy change. $\overrightarrow{I}_{seg}$, $\overrightarrow{\omega}_{seg}$, m_{seg} and $\overrightarrow{v}_{seg}$ are the inertia, the angular velocity, the mass and the linear velocity of the segment. Finally, P_{tot} is the external power.

To gain insight into the distribution of power over the individual body segments, segment powers were calculated for each segment based on solely kinematic data [38]. Power estimations based on solely kinematic data are usually less reliable than power estimations that are based on both kinematic and kinetic data [20]. Therefore, the segment power estimations in this study are used in addition to other power calculation methods with the purpose to gain insight into the power flow over the individual segments. The segment powers were calculated by taking the derivative of the sum of the potential and kinetic energies for each body segment, assuming 22 (N_s) rigid body segments (s) (Fig. 2.2) (Eq. 2.4-2.6). Total segment power was calculated by taking the sum of the individual segment powers (Eq. 2.7) [39].

$$E_{seg} = Eseg, pot + Eseg, kin_{rot} + Eseg, kin_{trans} \tag{2.4}$$

$$E_{seg} = m_{seg} g h_{seg} + \frac{1}{2} m_{seg} \overrightarrow{v}^2_{seg} + \frac{1}{2} I_{seg} \overrightarrow{\omega}^2_{seg} \tag{2.5}$$

$$\dot{E}_{seg} = \frac{dE_{seg}}{dt} \tag{2.6}$$

$$P_{seg} = \dot{E}_{seg} = \sum_{s}^{N_s} \dot{E}_{seg,s} \tag{2.7}$$

In equations 2.4-2.7, E_{seg}, $Eseg, pot$, $Eseg, kin_{rot}$ and $Eseg, kin_{trans}$ represent the total energy, the potential energy, the rotational kinetic energy and the translational kinetic energy of the segment. m_{seg}, h_{seg}, $\overrightarrow{v}_{seg}$, I_{seg} and $\overrightarrow{\omega}_{seg}$ are respectively the mass, the height, the linear velocity, the inertia and the angular velocity of the segment. g is the acceleration of gravity. Finally $\dot{E}_{seg}$ and P_{seg} are the individual segment and total segment powers.

The 22 segments were divided into subgroups. The subgroups ipsilateral and contralateral limb consisted of the femur, tibia, patella, talus, calcaneus, and toes of either the ipsilateral or the contralateral limb. The subgroup head-arms-trunk (HAT) consisted of the trunk, pelvis and the humerus, ulna, radius and hand of both arms.

Joint powers were calculated for each joint by taking the dot product of the joint moment and its angular velocity (Eq. 2.8). Total joint power was calculated by taking the sum of the individual joint powers, assuming 13 joints (the wrist, subtalar and mtp joints were locked).

$$P_j = \overrightarrow{M}_j \cdot \overrightarrow{\omega}_j \tag{2.8}$$

$$P_{joints} = \sum_{j}^{N_j} P_j \tag{2.9}$$

In equations 2.8-2.9, P_j is the individual joint power, $\overrightarrow{M}_j$ are the joint moments, $\overrightarrow{\omega}_j$ are the angular velocities around the joint and P_{joints} is the total joint power.

Muscle powers were derived from the OpenSim CMC outcomes.

Total work and individual segment, joint and muscle work can be calculated by integrating the power over a given time interval (Eq. 2.10). This was done to calculate the work over the complete time interval and for specific time frames within the gait cycle.

$$W = \int P dt \tag{2.10}$$

In equation 2.10, W is the work and P is the power.

2.2.3 Gait phases

As mentioned in section 2.2.1, due to the lack of a third force plate, gait data was analysed from the start of the midstance phase till the end of the gait cycle. The end of the gait cycle was characterized by heel strike of the ipsilateral limb. This was detected by the phase detection method that was developed by Zeni and colleagues [46]. With this method, heel strike is detected based on the position of the heel marker.

In the previous analysis, differences in total positive work between the two walking conditions were analysed for the complete gait cycle, but also for specific time intervals within the gait cycle, namely the rebound and the push-off phase [39]. The rebound and the push-off phase were defined based on the individual limb CoM power of the ipsilateral limb. The rebound phase was defined by the first period of positive individual limb CoM power, while the push-off phase was defined by the second period of positive individual limb CoM power [39]. In this study, it was attempted to analyse the work that was generated during the rebound and the push-off phase as well. However, it turned out that not for every trial it was possible to define the rebound phase based on the individual limb CoM power, because for some of the

trials the individual limb CoM power was not positive during this period (Fig. 2.4). Therefore, it was decided to compare the gait data of the two walking conditions for the midstance phase, defined as the period from the first peak in vertical ground reaction force till the first local minimum of this vertical ground reaction force [11], [37] (Fig. 2.5). The push-off phase was still defined by the positive individual limb CoM power in this study (Fig. 2.4).

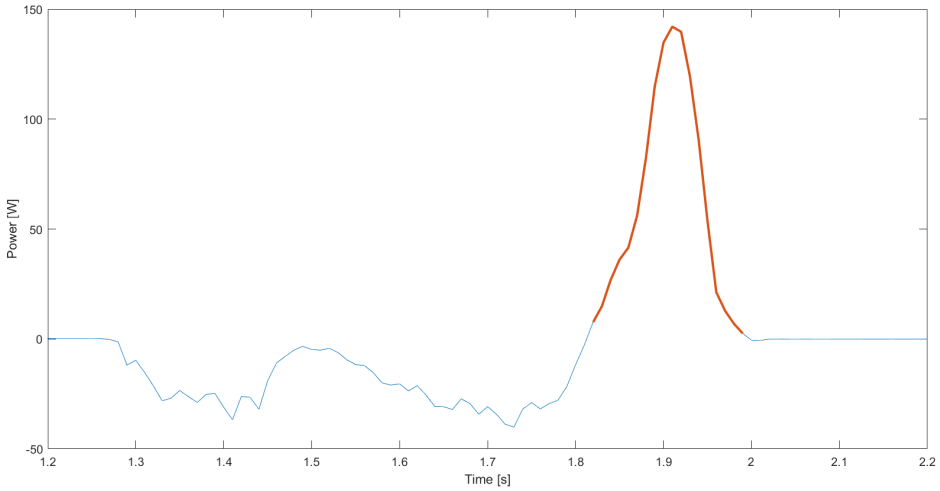

Figure 2.4: Individual limb CoM power of the ipsilateral limb. *The individual limb CoM power of the ipsilateral limb of one of the trials calculated with the unfiltered inverse kinematic results and the ground reaction force data. The red line shows the definition of the push-off phase: the time interval during the second part of the stance phase for which the individual limb CoM power is positive. As can be seen, no rebound phase could be determined for this trial based on the definition of positive individual CoM power during the first part of the stance phase, since the individual CoM power is not positive during the first part of the stance phase.*

2.2.4 Normalization

Walking speeds, powers and work were normalized to be able to compare the outcomes of different subjects with each other. The normalized walking speed was calculated with the following equation:

$$\hat{v} = v/\sqrt{gl_0} \tag{2.11}$$

in which $\hat{v}$ is the normalized walking speed, v is the measured walking speed is m/s, g is the acceleration of gravity in m/s^2 and l_0 is the leg length in m [10]. The leg length was calculated with the marker position data of the static trial and is defined as the vertical distance between the anterior superior iliac spine and the medial malleoli.

To calculate the normalized powers, the leg length of the subject, the mass of the subject and the acceleration of gravity must be taken into account. This leads to the following equation to calculate the normalized powers:

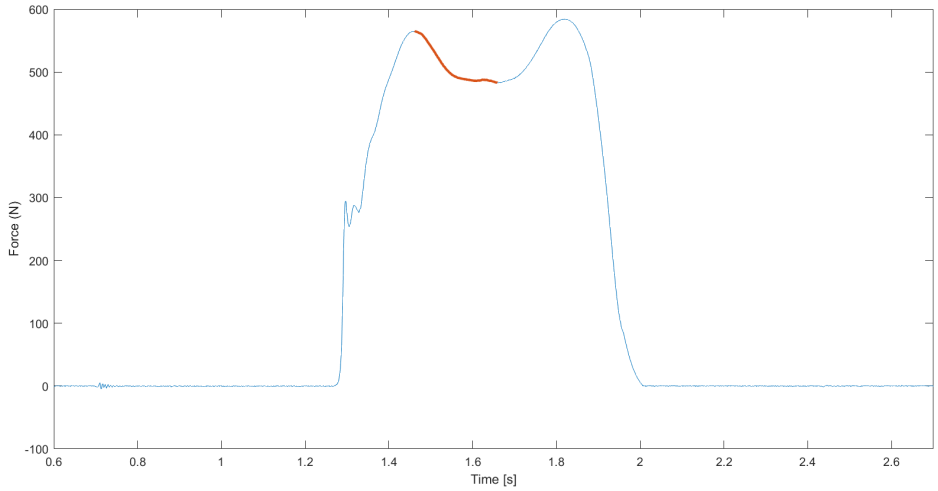

Figure 2.5: Definition of the midstance phase. *This figure shows the vertical component of the ground reaction force. The midstance phase is defined as the time interval from the first peak in vertical ground reaction force till the first local minimum of this vertical ground reaction force. The midstance phase is shown here in red.*

$$\hat{P} = \frac{P}{m_0 g^{3/2} l_0^{1/2}} \tag{2.12}$$

where $\hat{P}$ is the normalized power, P is the joint power in Watt, m_0 is the body mass in kg, g is the acceleration of gravity in m/s^2 and l_0 is the leg length in m [26].

The normalized work will also be calculated based on the leg length of the subject, the mass of the subject and the acceleration of gravity:

$$\hat{W} = \frac{W}{m_0 g l_0} \tag{2.13}$$

where $\hat{W}$ is the normalized work, W is the work in Joule, m_0 is the body mass in kg, g is the acceleration of gravity in m/s^2 and l_0 is the leg length in m [10].

2.2.5 Statistics

Normality was tested with a Kolmogorov-Smirnov test. Since the data was normally distributed, paired samples t-tests were performed to test the statistical significance of the differences between the two walking conditions.

Chapter 3

Results

The IK solutions show a good match between the model markers and the experimental markers. Mean total RMS errors for the normal walking and the trunk sway conditions are 0.98 ± 0.13 cm and 1.19 ± 0.27 cm respectively.

During the RRA step, residuals were reduced successfully. The average contribution of all the residuals together to the sum of the positive work generated by all joints and residuals was reduced to $1.52 \pm 0.85\%$ in the normal walking condition and $1.74 \pm 0.98\%$ in the trunk sway walking condition (Fig. 3.9). Average joint angle RMS errors of the RRA solutions with respect to the IK solutions were 0.26 ± 0.06 degrees and 0.40 ± 0.18 degrees for respectively the normal and trunk sway walking conditions.

The CMC results show an average contribution of the residuals and reserves together to the sum of the positive work generated by all muscles and the residuals and reserves of $2.49 \pm 0.89\%$ and $2.54 \pm 0.59\%$ for respectively the normal walking and the trunk sway condition (Fig. 3.12). Average joint angle RMS errors of the CMC solutions with respect to the RRA solutions were 0.13 ± 0.03 degrees for the normal walking condition and 0.11 ± 0.02 degrees for the trunk sway condition.

In figure 3.1, the mean lumbar bending angle of the trunk is shown for the normal and excessive trunk sway condition. A significant difference was found in the peak lumbar bending angle between the normal (9.35 ± 1.20 degrees) and the excessive trunk sway (22.52 ± 4.74 degrees) condition ($t(9)=-9.99$, $p<0.01$). This means that the subjects succeeded in walking with excessive medio-lateral trunk movements.

No significant difference was found in dimensionless walking speed between the normal walking (0.35 ± 0.02) condition and the trunk sway (0.36 ± 0.03) condition ($t(9)=-0.94$, $p=0.37$).

3.1 Total power and work

In figure 3.2 total body powers that are estimated in four different ways are depicted for the normal and trunk sway condition. Comparable power profiles were found for each method. However, especially during the push-off phase, the estimations of the external and total segment power were lower than the estimations

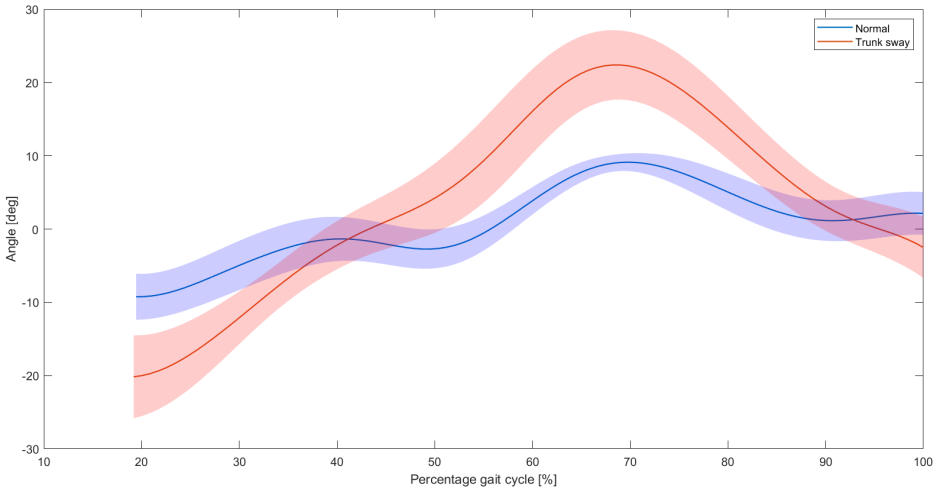

Figure 3.1: Lumbar bending angle. *The lumbar bending angle averaged over the ten subjects for the normal and trunk sway condition. The shaded area represents the standard deviation.*

of the total joint and total muscle power. This can be seen in figure 3.3 as well, where the positive work generated during the complete time interval and during the midstance and push-off phases calculated in four different ways are shown. A significant difference was found in positive work generated during the push-off phase estimated by the total joint power and the external power for the normal walking condition (external work: 0.02 ± 0.01, total joint work: 0.03 ± 0.01, $t(9)=-3.69$, $p<0.01$). Furthermore, a significant difference was found in positive work generated during midstance estimated by the total joint power and the external power for the normal walking condition (external work: 0.01 ± 0.00, total joint work: 0.01 ± 0.00, $t(9)=2.92$, $p<0.05$). No difference was found in the total positive work generated during the complete time interval estimated by the external work and the total joint work for the normal walking condition (external work: 0.05 ± 0.01, total joint work: 0.05 ± 0.01, $t(9)=-1.89$, $p=0.09$).

As can be seen in figure 3.4, the positive external work that was generated during midstance was higher for the trunk sway condition in comparison to the normal walking condition. However, this difference was non-significant (normal: 0.01 ± 0.00, trunk sway: 0.01 ± 0.01, $t(9)=-2.24$, $p=0.05$). Furthermore, no differences were found in the positive external work generated during the complete time interval (normal: 0.05 ± 0.01, trunk sway: 0.05 ± 0.02, $t(9)=-1.17$, $p=0.27$) and during the push-off phase (normal: 0.02 ± 0.01, trunk sway: 0.02 ± 0.01, $t(9)=2.21$, $p=0.05$).

3.2 Segment power and work

Positive total segment work generated during the midstance phase turned out to be significantly higher in the trunk sway (0.01 ± 0.01) condition in comparison to the normal walking (0.01 ± 0.00) condition ($t(9)=-2.30$, $p<0.05$). No differences were found in positive total segment work generated during the complete time interval

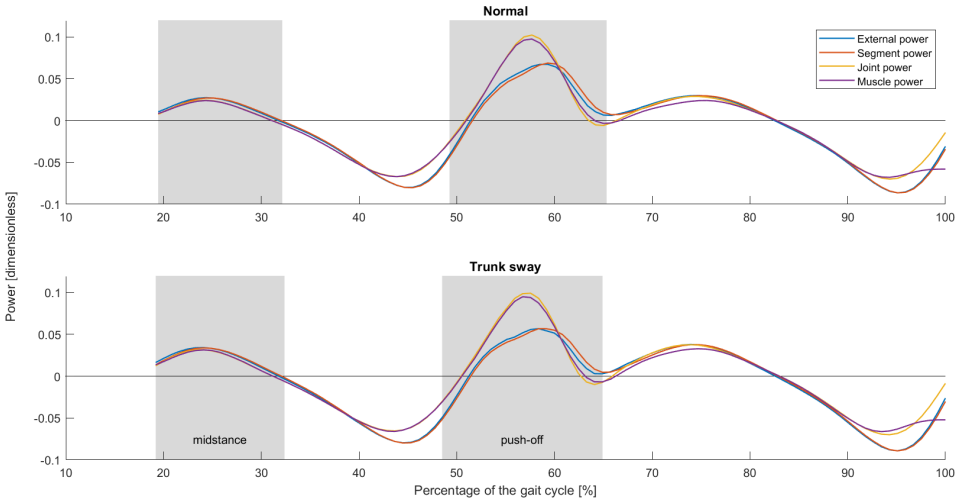

Figure 3.2: Total power. *The total power estimated in four different ways: external power, total segment power, total joint power and total muscle power.*

(normal: 0.05 ± 0.01, trunk sway: 0.05 ± 0.01, t(9)=-1.20, p=0.26) and during the push-off phase (normal: 0.02 ± 0.02, trunk sway: 0.02 ± 0.01, t(9)=2.19, p=0.06).

The individual segment powers are depicted in figure 3.5. For the head-arms-trunk (HAT) segment, a non-significant increase in total positive work was found for the trunk sway (0.02 ± 0.00) condition in comparison to the normal walking (0.02 ± 0.01) condition (t(9)=-1.77, p=0.11). Furthermore, there was no significant difference in total positive work generated by the ipsilateral limb (IL) between the normal walking (0.05 ± 0.01) condition and the trunk sway (0.05 ± 0.01) condition (t(9)=-0.77, p=0.46). Besides that, no significant difference in total positive work generated by the contralateral limb (CL) was found between the normal walking (0.01 ± 0.00) condition and trunk sway (0.01 ± 0.00) condition (t(9)=-1.61, p=0.14).

In figure 3.6, the contributions of the individual segments to the total work are depicted. As can be seen, an increase of the contribution of the HAT segment was found for the trunk sway condition. However, this increase was not tested to be significant (normal: $22.11 \pm 5.14\%$, trunk sway: $23.49 \pm 4.55\%$, t(9)=-1.47, p=0.17).

3.3 Joint power and work

Positive total joint work generated during the midstance phase was significantly higher during the trunk sway (0.01 ± 0.01) condition in comparison to the normal walking (0.01 ± 0.00) condition (t(9)=-2.45, p<0.05). Furthermore, a significant increase in positive total joint work generated during the complete time interval was found for the trunk sway (0.06 ± 0.02) condition in comparison to the normal walking (0.05 ± 0.01) condition (t(9)=-2.44, p<0.05). No significant difference was found in positive total joint work generated during the push-off phase (normal: 0.03 ± 0.01, trunk sway: 0.03 ± 0.01, t(9)=0.57, p=0.58).

The individual joint powers for the normal and excessive trunk sway condition are depicted in figure 3.7. The total positive work generated by the individual joints

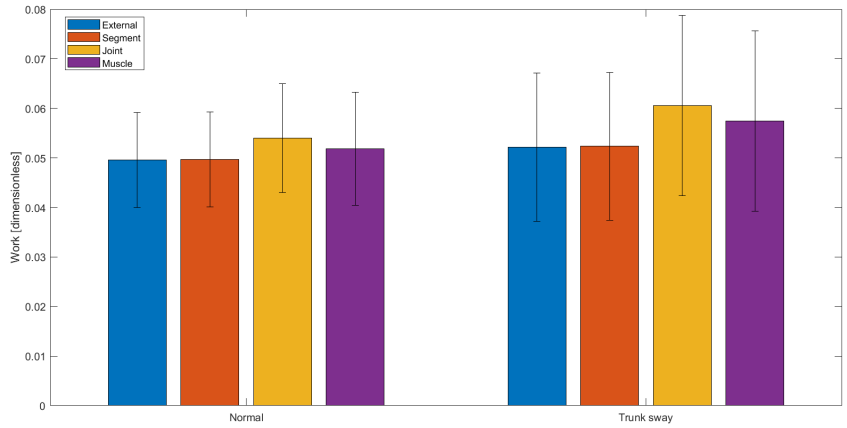

(a) Complete time interval

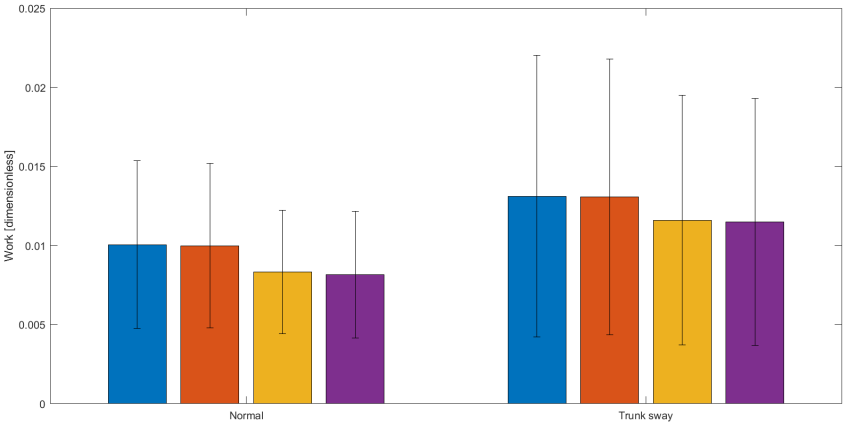

(b) Midstance

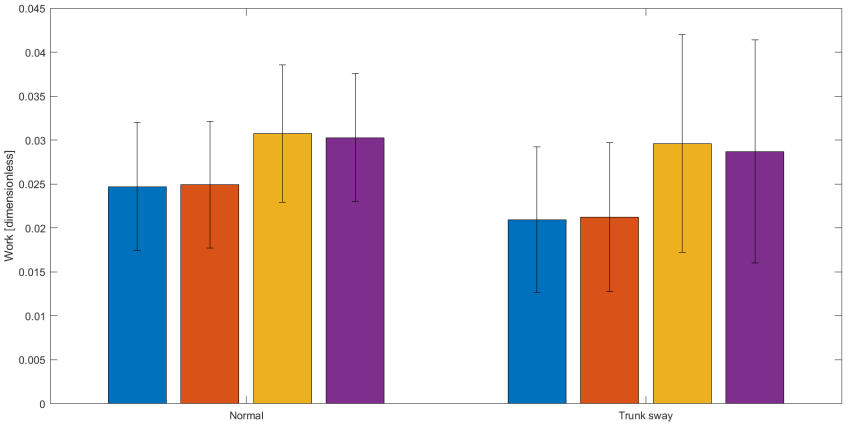

(c) Push-off

Figure 3.3: Total positive work. *The total positive work calculated from four different estimations of the total power: external power, total segment power, total joint power and total muscle power. The bars show the mean values ± standard deviation.*

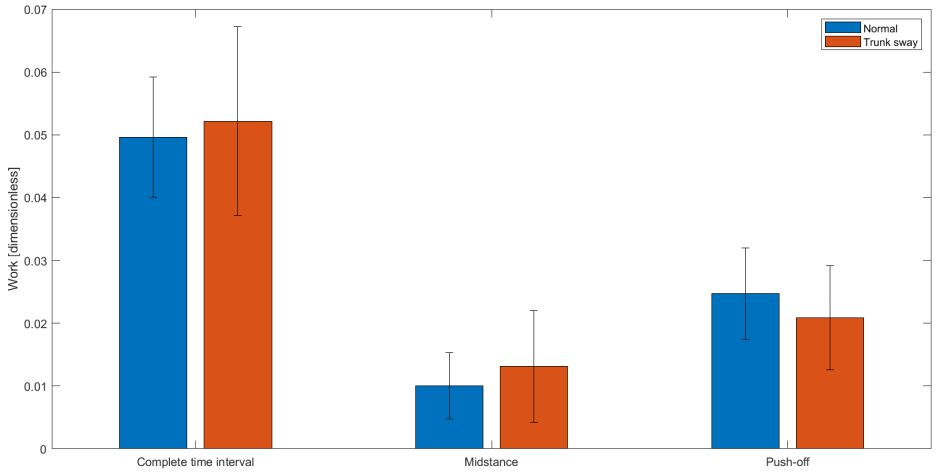

Figure 3.4: External work. *Positive work calculated from the external power. The bars show the mean values ± standard deviation.*

are depicted in figure 3.8. Total positive work at the lumbar joint increased for the excessive trunk sway (0.01 ± 0.01) condition in comparison to the normal walking (0.01 ± 0.00) condition ($t(9)=-4.18$, $p<0.01$), while there was no difference in positive work at the hip, knee and ankle joints of the ipsilateral limb between the two conditions (Hip: normal: 0.03 ± 0.01, trunk sway: 0.03 ± 0.01, $t(9)=-1.19$, $p=0.27$. Knee: normal: 0.00 ± 0.00, trunk sway: 0.01 ± 0.00, $t(9)=-1.15$, $p=0.28$. Ankle: normal: 0.03 ± 0.01, trunk sway: 0.03 ± 0.01, $t(9)=-1.12$, $p=0.29$). The increase in positive work at the lumbar joint over the complete time interval can be explained by an increase in positive work at the lumbar joint during midstance (normal: 0.00 ± 0.00, trunk sway: 0.00 ± 0.00, $t(9)=-3.06$, $p<0.05$).

The contributions of the individual joints to the total positive work are depicted in figure 3.9. As can be seen, the contribution of the lumbar joint to the total positive work increases (normal: $9.03 \pm 3.97\%$, trunk sway: $12.31 \pm 6.52\%$, $t(9)=-3.13$, $p<0.05$), while the contribution of the ankle joint of the ipsilateral limb decreases (normal: $32.48 \pm 6.00\%$, trunk sway: $30.42 \pm 6.66\%$, $t(9)=2.45$, $p<0.05$).

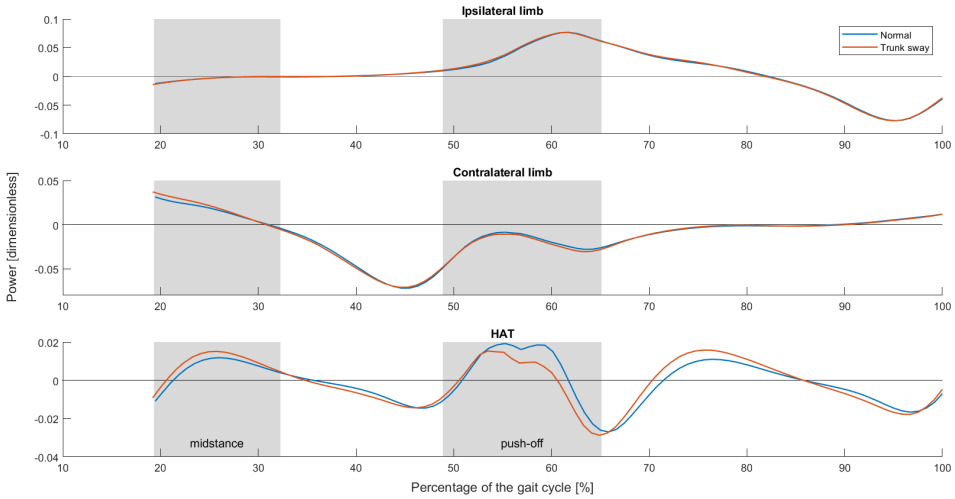

Figure 3.5: Segment power. *Segment powers for the segments: ipsilateral limb, contralateral limb and head-arms-trunk (HAT).*

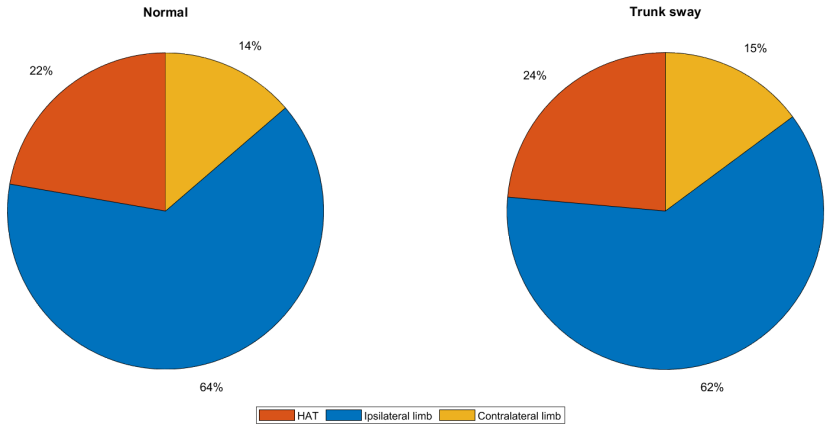

Figure 3.6: Segment work contributions. *Contributions of the individual segments: ipsilateral limb, contralateral limb and head-arms-trunk (HAT), to the total positive segment power.*

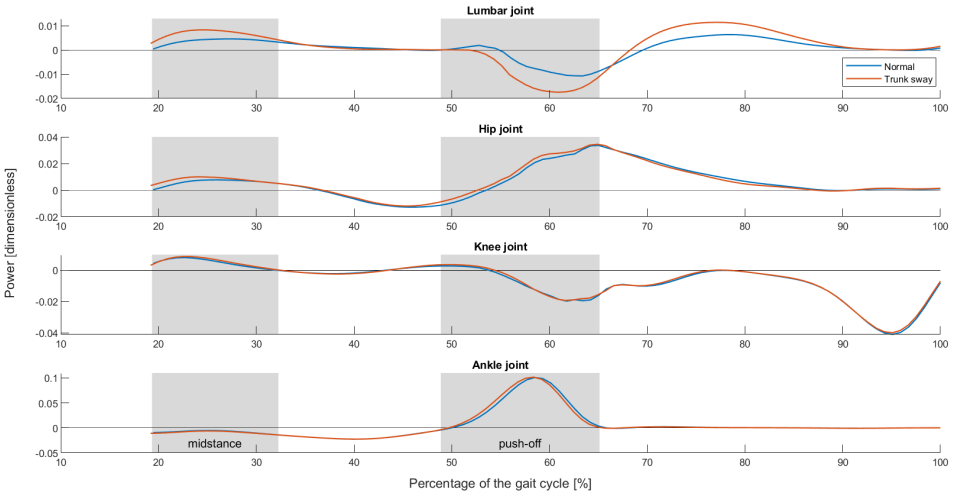

Figure 3.7: Joint power. *Joint powers of the lumbar joint and the hip, knee and ankle joints of the ipsilateral limb.*

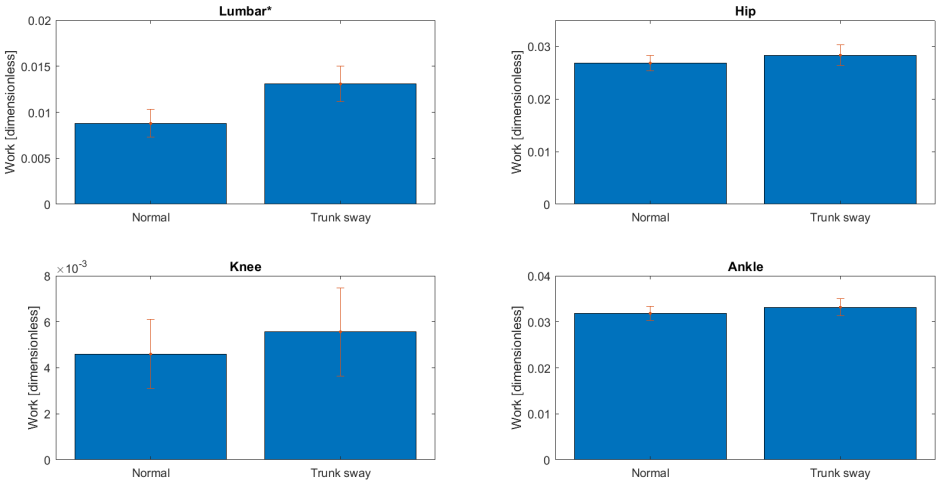

Figure 3.8: Joint work. *Positive work of the lumbar joint and the hip, knee and ankle joints of the ipsilateral limb. The bars show the mean values ± the total positive work generated by the residuals. Significant differences are indicated by *.*

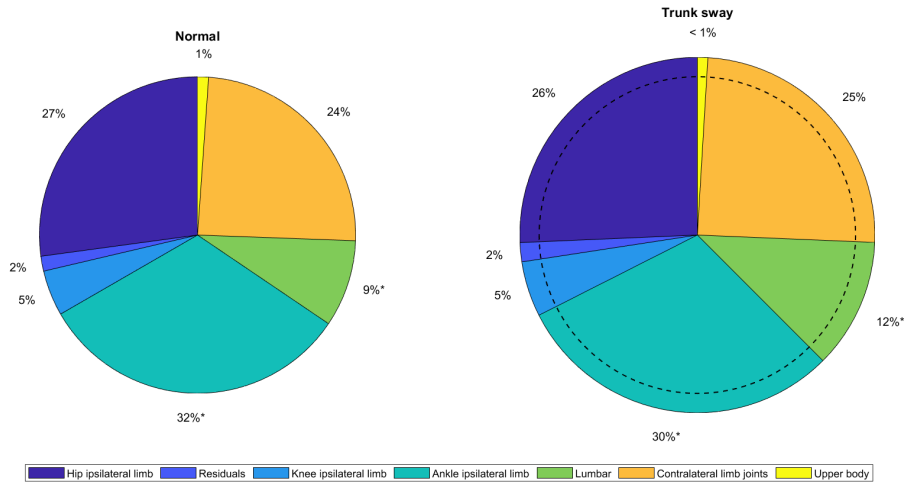

Figure 3.9: Joint work contributions. *Contributions of the individual joints and the residuals to the total positive joint work. Significant differences are indicated by *. The surface area represents the positive total joint work. A significant increase in positive total joint work in the trunk sway condition is indicated by the dashed line.*

3.4 Muscle power and work

Positive total muscle work generated during the midstance phase was significantly higher for the trunk sway (0.01 ± 0.01) condition in comparison to the normal walking (0.01 ± 0.00) condition ($t(9)=-2.55$, $p<0.05$). No significant differences were found in positive total muscle work generated during the complete time interval (normal: 0.05 ± 0.01, trunk sway: 0.06 ± 0.02, $t(9)=-2.13$, $p=0.06$) and during the push off phase (normal: 0.03 ± 0.01, trunk sway: 0.03 ± 0.01, $t(9)=0.72$, $p=0.49$).

Thirteen muscles showed a significant difference in total positive work between the normal and trunk sway condition (Table 3.2). The total positive work generated by those muscles in both conditions is depicted in figure 3.10. As can be seen, the greatest increase in positive work was found for the lumbar bending muscles.

In figure 3.11, the muscle powers of the muscles that showed the greatest significant increase in muscle work during the trunk sway condition are shown. As can be seen, the positive power generated by the lumbar bending muscles increased during midstance and more negative power was generated during the push-off phase.

The contributions to the total power generation of the muscles that showed the greatest significant increase in muscle work during the trunk sway condition are shown in figure 3.12. A clear increase in the contribution to the total positive work of the lumbar bending muscles was found for the trunk sway condition (normal: $2.43 \pm 0.84\%$, trunk sway: $3.33 \pm 1.56\%$, $t(9)=-3.14$, $p<0.05$). Furthermore, a significant increase in the contribution to the total positive work of the semimembranosus muscle of the ipsilateral limb was found (normal: $1.65 \pm 0.46\%$, trunk sway: $1.80 \pm 0.46\%$, $t(9)=-4.31$, $p<0.01$). No differences in the contributions of the other muscles were found.

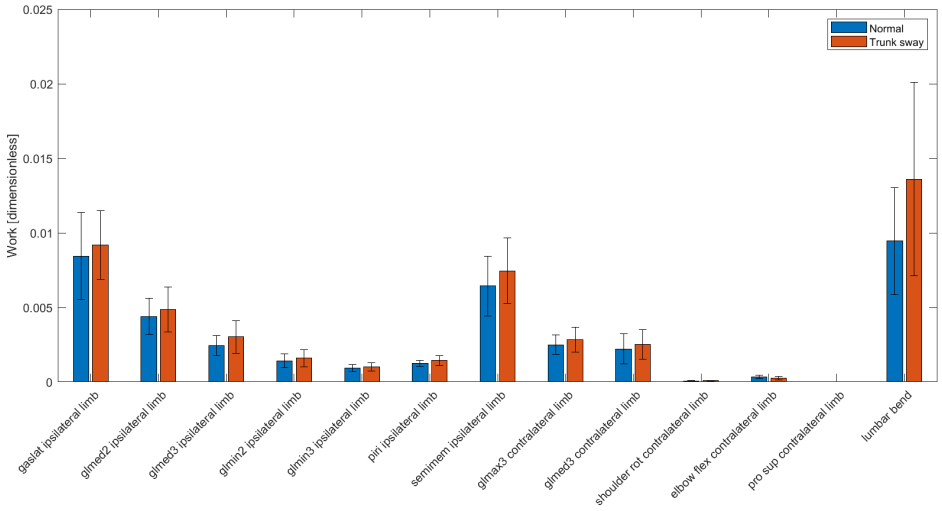

Figure 3.10: Muscle work. *Total positive work of the muscles that showed a significant increase or decrease during the trunk sway condition. The bars show the mean values ± standard deviation. A list of the used abbreviations for the muscle names can be found in appendix C.*

3.5 Effect of residuals

The effect of the residual forces and moments on the power outcomes are investigated by comparing the powers calculated with the angular velocities and joint moments before and after reducing the residuals. In figure 3.13 the total joint powers calculated before and after reducing the residuals are depicted. As can be seen, the decrease in positive total joint work during the push-off phase was higher before the residuals were reduced in comparison to after the residuals were reduced (decrease of 10.59% and 3.58% respectively). However, the reduction in positive total joint work during the push-off phase calculated with the joint angles and joint moments before the residuals were reduced was still non-significant (normal: 0.02 ± 0.01, trunk sway: 0.02 ± 0.01, $t(9)=1.47$, $p=0.18$).

This same trend can be found when looking at the ankle power calculated with the angular velocities and joint moments before and after reducing the residuals (Fig. 3.14). While an increase of 2.64% in positive ankle work generated during the push-off phase was found after reducing the residuals, a decrease of 1.18% in positive ankle work generated during the push-off phase before reducing the residuals was found. This decrease in the trunk sway condition in comparison to the normal walking condition was non-significant (normal: 0.03 ± 0.00, trunk sway: 0.03 ± 0.01, $t(9)=0.21$, $p=0.84$).

For the lumbar, hip and knee joints, no differences were found in the inequalities between the normal walking condition and the trunk sway condition in power calculated with the joint angles and joint moments before and after reducing the residuals.

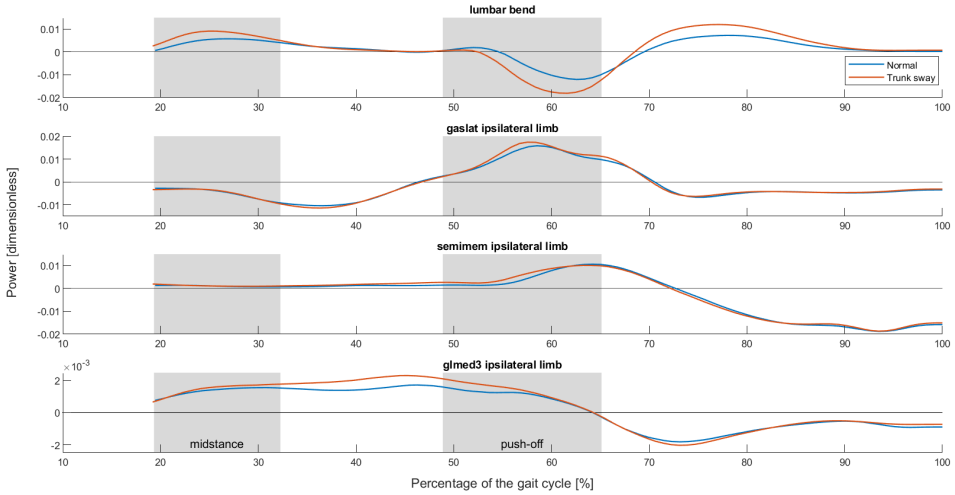

Figure 3.11: Muscle power. *Power generated by the muscles that showed the greatest significant increase or decrease in positive work generation during the trunk sway condition. A list of the used abbreviations for the muscle names can be found in appendix C.*

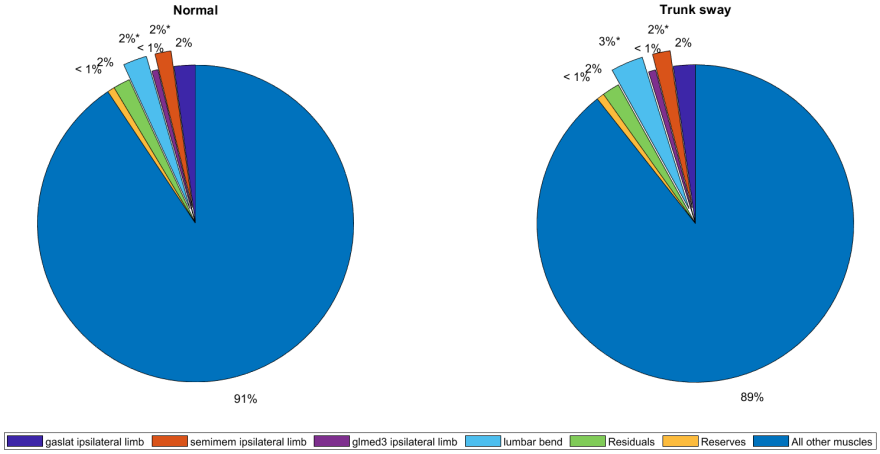

Figure 3.12: Muscle work contributions. *Contributions of the individual muscles that showed the greatest significant increase or decrease in generated positive work and the residuals and reserves to the total positive work. Significant differences are indicated by *. A list of the used abbreviations for the muscle names can be found in appendix C.*

Table 3.1: Total positive muscle work. *Mean values ± standard deviation of the positive work generated by the thirteen muscles that showed a significant increase or decrease during the trunk sway condition. The outcomes of the paired samples t-tests are shown in the fourth column. A list of the used abbreviations for the muscle names can be found in appendix C. The positive work during the trunk sway condition and the normal walking condition generated by these thirteen muscles is depicted in figure 3.10.*

Muscle	Mean value normal walking condition	Mean value trunk sway walking condition	t-test
gaslat ipsilateral limb	0.0085 ± 0.0029	0.0092 ± 0.0023	t(9)=-2.28, p<0.05
glmed2 ipsilateral limb	0.0044 ± 0.0012	0.0049 ± 0.0015	t(9)=-2.83, p<0.05
glmed3 ipsilateral limb	0.0024 ± 0.0007	0.0030 ± 0.0011	t(9)=-2.50, p<0.05
glmin2 ipsilateral limb	0.0014 ± 0.0005	0.0016 ± 0.0006	t(9)=-2.36, p<0.05
glmin3 ipsilateral limb	0.0009 ± 0.0002	0.0010 ± 0.0003	t(9)=-4.29, p<0.01
piri ipsilateral limb	0.0012 ± 0.0002	0.0014 ± 0.0003	t(9)=-2.77, p<0.05
semimem ipsilateral limb	0.0064 ± 0.0020	0.0074 ± 0.0022	t(9)=-5.48, p<0.01
glmax3 contralateral limb	0.0025 ± 0.0007	0.0028 ± 0.0008	t(9)=-3.22, p<0.05
glmed3 contralateral limb	0.0022 ± 0.0010	0.0025 ± 0.0010	t(9)=-2.80, p<0.05
shoulder rot contralateral side	0.0001 ± 0.0000	0.0001 ± 0.0000	t(9)=-2.33, p<0.05
elbow flex contralateral side	0.0003 ± 0.0001	0.0003 ± 0.0001	t(9)= 2.82, p<0.05
pro sub contralateral side	0.0000 ± 0.0000	0.0000 ± 0.0000	t(9)=-3.11, p<0.05
lumbar bend	0.0095 ± 0.0036	0.0136 ± 0.0065	t(9)=-3.80, p<0.01

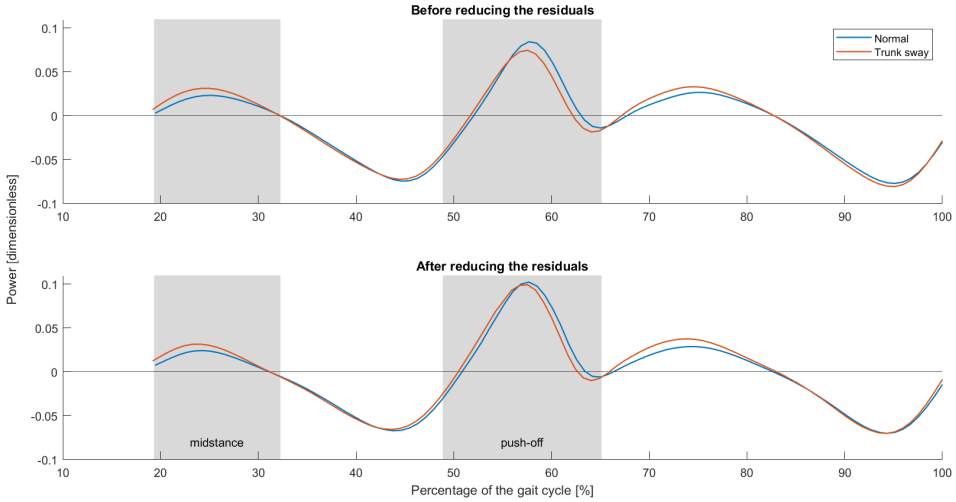

Figure 3.13: Total joint power before and after the residuals were reduced. *The total joint power for the trunk sway condition and the normal walking condition before and after the residual reduction algorithm was applied.*

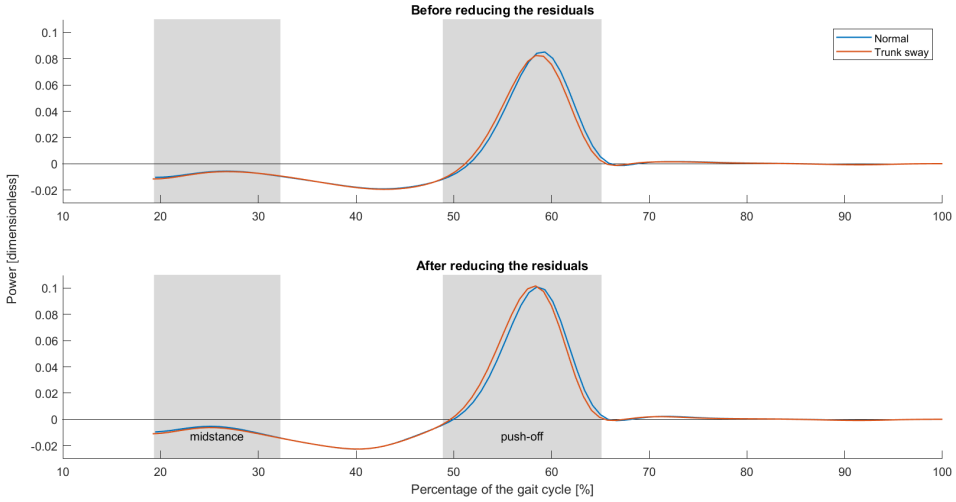

Figure 3.14: Ankle joint power before and after the residuals were reduced. *The ankle joint power of the ipsilateral limb for the trunk sway condition and the normal walking condition before and after the residual reduction algorithm was applied.*

Chapter 4

Discussion

The first aim of this study was to evaluate the validity of the results obtained by a previous analysis. This previous analysis found a significant increase of 192% in positive work generated during the rebound phase and a significant decrease of 28.2% in positive work generated during the push-off phase. This was attributed to an increase of 10.8% in positive work generated at the hip joint and a decrease of 11% in positive work generated at the ankle joint. Furthermore, an increase of 315% in positive work generated at the lumbar joint was found [39]. However, these results are totally not in line with the findings of the current study. In this study, a significant increase of 48.78% in total positive work at the lumbar joint was found, but no differences in total positive work at the hip, knee and/ or ankle joints were found. Since the same data set is used in both studies, this remarkable discrepancy certainly requires attention.

Firstly, it must be noted that hardly any information about the validity of the outcomes is provided in the previous analysis. The only sentence in the whole article that says something about the validity of the outcomes is: "Our estimates for normal gait were in reasonable agreement with prior literature reporting total body power estimates for ipsilateral limb and whole body." [39]. However, it remains unknown what was meant by 'reasonable'. No additional analyses or figures to support this statement were provided in the article. Furthermore, no measures that say something about how good the IK results match the marker data were reported. Moreover, no information can be found in the article about the residual forces and moments of the inverse dynamic results. It is suggested that the latter could be causing the discrepancy in outcomes between both studies.

An important difference between the current study and the study of van der Ploeg is the way in which it was dealt with the residuals. In the current study, residual forces and moments were reduced to make the kinematic outcomes more dynamically consistent with the experimentally measured ground reaction forces and moments. In the study of van der Ploeg, the residuals were not reduced [39]. Residual forces and moments are non-physical compensatory forces and moments that account for dynamic inconsistencies between the joint accelerations estimated from the experimental markers and the ground reaction force data. The inconsistencies can be caused by errors in marker data or ground reaction force data or by inaccuracies of the scaled model in terms of geometry and mass distributions. Hence, the residuals represent the errors in the joint angle and joint moment outcomes [28]. Therefore, it

is important to reduce the residual forces and moments as much as possible. Since the residuals were not reported in the study of van der Ploeg, no conclusions can be drawn on the presence of errors in the outcomes [39]. However, it is assumed that the residuals did have a significant contribution to the power and work outcomes. This means, the errors in inverse kinematic and inverse dynamic outcomes in the study of van der Ploeg could be accountable for the discrepancy in the results of both studies. This assumption is supported by the effect of the residuals on the power outcomes as was analysed in the current study. As mentioned in the results chapter, although an increase of 2.64% in positive ankle work generated during the push-off phase was found after reducing the residuals, a small decrease of 1.18% in positive ankle work generated during the push-off phase was found when using the joint angles and joint moments before the residuals were reduced. However, this decrease in positive ankle work calculated with the joint angles and moments before the residuals were reduced is still very small with respect to the decrease in positive ankle work that was found by the previous analysis (1.18% and 11% respectively). It is suggested that this could be caused by higher residuals in the previous analysis. One of the reasons for that could be the replication of the ground reaction forces and moments. In this study it was decided not to replicate the ground reaction forces and moments, because this led to an excessive increase of the residuals over the gait cycle. It is unknown how the ground reaction forces and moments were replicated exactly in the previous analysis and how this affected the residuals. Nevertheless, the effect of the residuals on the ankle power outcomes in the current study support the suggestion that the discrepancy in outcomes of both studies could be caused by high residual forces and moments in the study of van der Ploeg. However, no definite conclusion can be drawn on this, since the residuals are not reported in the article of van der Ploeg.

In both the current and the previous analysis, a musculoskeletal model is used to obtain the kinematic and kinetic outcomes. During the analyses, the model is driven such that it tracks the experimental motion data as good as possible [4]. In this way, the results are always in compliance with the musculoskeletal model. This also means, the kinematic and kinetic outcomes are strongly dependent on the underlying model that is used and therefore the validity of the outcomes is dependent on the validity of the model itself. Hence, it is important to mention that many assumptions are made in the development of the models [4]. Furthermore, the musculoskeletal models represent the average human body and although the models are scaled for every subject, the models do not account for detailed individual differences in musculoskeletal characteristics. Moreover, Roelker and colleagues showed that using a different musculoskeletal model could lead to differences in kinematic and kinetic outcomes [31]. Hence, the differences in outcomes between the current and the previous analysis could be caused by differences in the musculoskeletal models. This highlights the importance of the validation of the musculoskeletal models that are used in the data analyses. Since no comprehensive validation studies have been done yet, more research, including a sensitivity analysis to test the effect of the model parameters on the outcomes, is needed to investigate the fidelity of the models that were used in the current and the previous analysis [9].

So due to a lack of reported residuals, errors in the IK solutions and other fidelity measures, it is hard to say anything about the validity of the results of the study of

van der Ploeg. However, we can say something about the validity of the results of the current study. As mentioned in the results chapter, the residual forces and moments contribute for 1.63% to the sum of the positive work generated by all the joints and the residuals. In figure 3.8, the positive work generated by the individual joints is depicted. The error bars that are shown in this figure represent the total positive work generated by all the residuals in both walking conditions. As can be seen in the figure, the difference in lumbar work between the two walking conditions is bigger than the total positive work generated by the residuals (difference in dimensionless lumbar work: 0.0043, residual work normal and trunk sway condition: 0.0015 and 0.0019). Therefore, it can be concluded that the residuals are not influencing the conclusions that can be drawn out of the differences in positive lumbar work between the two walking conditions.

In terms of muscle work however, the residuals and reserves do contribute for a significant amount to the total positive work. As mentioned in the results chapter, the residual and reserve forces and moments contribute for 2.52% to the sum of the positive work generated by all muscles and the residuals and reserves. Although this value seems to be low, the amount of positive work generated by the residuals and reserves is still quite big with respect to the differences in positive muscle work between the two walking conditions, since the amount of work generated by the individual muscles is only small. For example, the difference in normalized work generated by the lumbar bending muscles between the two walking conditions is 0.0041, while the normalized work generated by the residuals and reserves is 0.0096 in the normal walking condition and 0.0105 in the trunk sway condition. This means, it is hard to validate the muscle power and work results, since the differences in muscle work between the two conditions could potentially be caused by errors in kinematic and dynamic results represented by the residual and reserve forces and moments. Therefore, it is suggested for future research to measure electromyographic (EMG) patterns and use this data for the validation of the simulated muscle activations by comparing the simulated muscle activations with the EMG recordings [7]. Moreover, the EMG recordings could be used as an input for an EMG-driven musculoskeletal model [40], [19]. The muscle forces that can be obtained in this way can be compared with the muscle forces derived from the simulation.

The kinematic and kinetic outcomes of this study were compared to prior literature reporting joint angles and joint moments for a slow walking speed. The comparison can be found in appendix D. As can be seen, the joint angles of this study match the joint angles reported by prior literature well. The peak values in joint angles that were found in this study are in line with the peak values found by prior studies (less than 3 degrees difference in comparison to at least one of the articles with which the results are compared). The only exception is the peak hip extension angle, which is found to be at least 8 degrees higher in comparison to what was reported by the articles with which it has been compared. When looking at the joint moments, joint moment profiles and peak values found for the hip, knee and ankle joint were comparable to prior literature (less than 0.3 Nm/kg difference in comparison to at least one of the articles with which the results are compared). However, since gait kinematics and kinetics are strongly dependent on walking speed, subject characteristics and even research methodology, it is difficult to compare the gait kinematics and kinetics of different studies and therefore the comparison with

prior literature is of limited value.

When looking at the results of the current study and the results as reported by van der Ploeg, another thing must be noted. In the study of van der Ploeg it is concluded that when healthy people walk with excessive medio-lateral trunk movements, the human musculoskeletal system compensates for the increase in lumbar work by a decrease in ankle work [39]. However, the reduction in ankle work that was found in the study of van der Ploeg was not even a statistical significant reduction. His conclusion about the reduction in ankle work was based on a statistical significant decrease of positive external work generated during the push-off phase. Since the ankle plantar flexors are the main contributors to the power generation during the push-off phase and because a (non-statistical significant) reduction in ankle work was found during this push-off phase, it was concluded that the ankle muscles were responsible for the decrease in positive work during the push-off phase. However, since the difference in ankle work between the two walking conditions was not even a statistical significant difference, it is not really appropriate to conclude that there is a real reduction in ankle push-off power based on these results. Thus, the results of the analysis by van der Ploeg and the results of the current analysis are maybe more in line with each other than originally thought.

A limitation of the current study is that linear actuators about the lumbar joint were used in the musculoskeletal model in OpenSim instead of actual trunk muscles. It is hypothesized that muscles, including multi-articular muscles, are responsible for the transfer of power between joints, segments and planes because of their complex interaction with the dynamics of the body segments [45]. Therefore, to obtain a more realistic insight into the power flow of the body, it would be valuable to add trunk muscles to the model. The use of linear actuators implies that the actuators are spanning only one joint, in one segment, in one plane, which is a highly simplified representation that affects the simulated muscle interactions. Hence, it is recommended for future research to include trunk muscles in the OpenSim model to get a more realistic insight into the power flow between joints, segments and planes.

Furthermore, as mentioned in the results chapter, significant differences in positive work were found between the external and total joint work estimations for the midstance and push-off phase. This is important to mention, because in theory all four estimations of positive work should be the same. Therefore, if no significant differences would have been found between the different estimations of positive work, this would have supported the accuracy of the outcomes. It is suggested that the difference in power estimated by the external and total segment power and the total joint and muscle power is caused by an incorrect estimation of the rotational kinetic energy, because both the external and total segment power estimations are dependent on capturing the rotational kinetic energy. However, as can be seen in figure 3.3, the same trends were observed for all four estimations of the positive work during the complete time interval, the midstance and the push-off phase when comparing the normal walking condition to the excessive trunk sway condition. This indicates that although there are significant differences in the positive work calculated by the different methods, all estimations show the same effect of excessive medio-lateral trunk movements on the positive power generated during walking.

Another point that must be noted is that the recommended mass adjustments and the location of the CoM were adjusted manually after running the RRA tool in OpenSim. This was done because the recommended mass adjustments as well as the adjustment of the location of the CoM were applied in the wrong direction by OpenSim. It is unknown what caused these incorrect adjustments by OpenSim, but after experiencing this, this bug was reported on the OpenSim website and mass adjustments and CoM location changes were applied manually to avoid mistakes.

When looking at the results of this study, an increase in total positive lumbar joint work was found for the trunk sway condition in comparison to the normal walking condition. This can be explained by an increase in positive lumbar joint work during midstance. The increase in power generated at the lumbar joint causes an increase in the contribution of the lumbar joint to the total positive joint work, while the contribution of the ankle joint decreased due to this increase in power generation at the lumbar joint. These differences between the normal and trunk sway conditions can be explained by an increase in power generated by the lumbar bending muscles, which causes an increase in the contribution of the lumbar bending muscles to the total positive muscle work. Furthermore, a significant increase in the contribution of the semimembranosus muscle of the ipsilateral limb to the total positive muscle work was found. In summary, the lumbar bending muscles seem to be responsible for the increased lumbar bending angles during walking with excessive medio-lateral trunk movements, since the power generated by the lumbar bending muscles increased during the phases at which the peak lumbar bending angles occurred. This is causing an increase in power generated at the lumbar joint and thereby an increase in the contribution of the lumbar joint to the total positive power. The increase in the power generated by the semimembranosus can possibly also be explained by the excessive trunk movements in the frontal plane. During the push-off phase, the CoM of the body is accelerated laterally [25]. One of the muscle groups that is contributing to this lateral acceleration is the hip adductor group [25]. Since the semimembranosus muscle is besides extension of the hip and flexion of the knee also responsible for adduction of the hip when the hip is abducted [3], [36], the semimembranosus can contribute to the lateral acceleration of the CoM during the push-off phase of walking. In this way, the semimembranosus of the ipsilateral limb can contribute to the movements of the CoM in the frontal plane and thereby to the medio-lateral movements of the trunk.

The second aim of this study was to uncover the underlying biomechanical compensatory mechanisms of walking with excessive medio-lateral trunk movements. It was supposed that this could contribute to the determination of appropriate treatment of patients with reduced calf muscle strength and that this could be valuable for the development of assistive devices. However, this study found no relationship between medio-lateral trunk movements and ankle push-off power in healthy subjects walking with excessive medio-lateral trunk movements. This means, no compensatory mechanisms were identified in this study that could contribute to our understanding of compensatory mechanisms that are used by patients with reduced calf muscle strength. One of the reasons why there were not any compensation mechanisms identified in this study might be that this method of investigation with healthy subjects is not suitable to gain insight into compensation strategies as used by patients with calf muscle weakness. This can be due to the fact that the subjects in this

study had a lot of freedom in how to make the excessive trunk movements exactly. This led to a great variability in trunk movements (mean peak lumbar bending angle ± standard deviation in the trunk sway condition: 22.52 ± 4.74 degrees). Some people swayed unevenly, while others changed the timing of their trunk movements every trial [39]. For compensation strategies, the timing and the amplitude of the compensatory movements are really important [23]. When the compensatory movements are not timed adequately, the movements do not lead to a compensation of a certain deficit, but the movements only lead to an aggravation of the impairments. Therefore, it could be that due to this great variability in trunk movements, no effect of the excessive trunk movements was found on the power generated at the leg joints and thus this method of investigation might not be suitable for gaining insight into compensation strategies as used by patients with calf muscle weakness.

Moreover, a great variability in walking speed was found as well. Although no significant difference in walking speed was found between the trunk sway condition and the normal walking condition, differences in walking speed between the two conditions for individual subjects were up to 9.82%. Therefore, it is recommended for future research to control the walking speed more strictly to decrease inter- and intrasubject variability, for example by using a metronome.

Since research with patients makes it difficult to distinguish between primary deviations in muscle activation patterns caused by the underlying pathologies and secondary deviations due to the applied compensation strategies, research with healthy subjects could be valuable in obtaining insight into the applied compensation strategies. In this study, the effect of an experimental manipulation of the trunk on the power generated at the ankle joint was studied. Future research could investigate the effect of a manipulation at the ankle joint on the trunk segment. Simulating reduced calf muscle strength at healthy subjects, by for example limiting the degrees of freedom of the ankle joint, and comparing this to normal, free walking, could tell us something about the compensation strategies that can be used to overcome reduced calf muscle strength. When comparing the outcomes to observations of pathological gait, primary and secondary deviations in muscle activation patterns can be distinguished which could lead to a better understanding of the compensation strategies that are used by patients with reduced calf muscle strength.

Chapter 5

Conclusion

The first aim of this study was to evaluate the validity of the results obtained by a previous analysis. However, the results of this study contrast those of the previous analysis by van der Ploeg [39]. The findings of the current study were in agreement with prior literature and showed good accuracy by low tracking errors and low residuals. It is suggested that the discrepancy between the outcomes of the two studies is caused by high residual forces and moments in the study of van der Ploeg. However, no conclusions can be drawn on the exact nature of the differences, since no information about the residuals is provided in the article of van der Ploeg [39]. Nevertheless, by revealing the discrepancy between the results of both studies, this study highlights the importance of the validation of results.

The second aim of this study was to uncover the underlying biomechanical compensatory mechanisms of walking with excessive medio-lateral trunk movements. An increase in positive work at the lumbar joint was found, but no differences in positive work at the hip, knee and/ or ankle joints were found when comparing the trunk sway condition to the normal walking condition. The lumbar bending muscles turned out to be responsible for the increase in positive work at the lumbar joint. In conclusion, we did not find medio-lateral trunk sway to be a compensatory mechanism for ankle plantar flexor weakness. Therefore, more research is needed to understand why trunk sway is commonly observed in patients with reduced plantar flexion muscle strength.

Bibliography

[1] M. Attias, A. Bonnefoy-Mazure, M. Lempereur, P. Lascombes, G. De Coulon, and S. Armand. Trunk movements during gait in cerebral palsy. *Clinical Biomechanics*, 30(1):28–32, 2015.

[2] Å. Bartonek, H. Saraste, M. Eriksson, L. Knutson, and A.G. Cresswell. Upper body movement during walking in children with lumbo–sacral myelomeningocele. *Gait & posture*, 15(2):120–129, 2002.

[3] D. Colgan, P. Trench, D. Slemon, D. McTague, J.B. Finlay, P. O'Donnell, and E.G. Little. A review of joint and muscle load simulation relevant to in-vitro stress analysis of the hip. *Strain*, 30(2):47–62, 1994.

[4] S.L. Delp, F.C. Anderson, A.S. Arnold, P. Loan, A. Habib, C.T. John, E. Guendelman, and D.G. Thelen. Opensim: open-source software to create and analyze dynamic simulations of movement. *IEEE transactions on biomedical engineering*, 54(11):1940–1950, 2007.

[5] C.A. Fukuchi, R.K. Fukuchi, and M. Duarte. A public dataset of overground and treadmill walking kinematics and kinetics in healthy individuals. *PeerJ*, 6:e4640, 2018.

[6] E.M. Gutierrez, Å. Bartonek, Y. Haglund-Åkerlind, and H. Saraste. Characteristic gait kinematics in persons with lumbosacral myelomeningocele. *Gait & posture*, 18(3):170–177, 2003.

[7] S.R. Hamner, A. Seth, and S.L. Delp. Muscle contributions to propulsion and support during running. *Journal of biomechanics*, 43(14):2709–2716, 2010.

[8] G.G. Handsfield, C.H. Meyer, M.F. Abel, and S.S. Blemker. Heterogeneity of muscle sizes in the lower limbs of children with cerebral palsy. *Muscle & nerve*, 53(6):933–945, 2016.

[9] J.L. Hicks, T.K. Uchida, A. Seth, A. Rajagopal, and S.L. Delp. Is my model good enough? best practices for verification and validation of musculoskeletal models and simulations of movement. *Journal of biomechanical engineering*, 137(2), 2015.

[10] A.L. Hof. Scaling gait data to body size. *Gait & posture*, 3(4):222–223, 1996.

[11] E. Kessler, P.A. Tarazaga, and R. Queen. Defining groupings and classification of human gait using correlation of ground reaction force measurements. In *Dynamics of Civil Structures, Volume 2*, pages 377–384. Springer, 2019.

[12] D. Kiernan, R. O'Sullivan, A. Malone, T. O'Brien, and C.K. Simms. Pathological movements of the pelvis and trunk during gait in children with cerebral palsy: a cross-sectional study with 3-dimensional kinematics and lower lumbar spinal loading. *Physical therapy*, 98(2):86–94, 2018.

[13] B.K. Krautwurst, S.I. Wolf, D.W.W. Heitzmann, S. Gantz, F. Braatz, and T. Dreher. The influence of hip abductor weakness on frontal plane motion of the trunk and pelvis in patients with cerebral palsy. *Research in developmental disabilities*, 34(4):1198–1203, 2013.

[14] D.J. Kuhman and C.P. Hurt. Lower extremity joints and muscle groups in the human locomotor system alter mechanical functions to meet task demand. *Journal of experimental biology*, 222(20):jeb206383, 2019.

[15] A. Lamontagne, F. Malouin, C.L. Richards, and F. Dumas. Mechanisms of disturbed motor control in ankle weakness during gait after stroke. *Gait & posture*, 15(3):244–255, 2002.

[16] C.L. Lewis and D.P. Ferris. Walking with increased ankle pushoff decreases hip muscle moments. *Journal of biomechanics*, 41(10):2082–2089, 2008.

[17] S.W. Lipfert, M. Günther, D. Renjewski, and A. Seyfarth. Impulsive ankle push-off powers leg swing in human walking. *Journal of experimental biology*, 217(8):1218–1228, 2014.

[18] M.Q. Liu, F.C. Anderson, M.H. Schwartz, and S.L. Delp. Muscle contributions to support and progression over a range of walking speeds. *Journal of biomechanics*, 41(15):3243–3252, 2008.

[19] D.G. Lloyd and T.F. Besier. An emg-driven musculoskeletal model to estimate muscle forces and knee joint moments in vivo. *Journal of biomechanics*, 36(6):765–776, 2003.

[20] P.E. Martin, G.D. Heise, and D.W. Morgan. Interrelationships between mechanical power, energy transfers, and walking and running economy. *Medicine and science in sports and exercise*, 25(4):508–515, 1993.

[21] B.F. Mentiplay, M. Banky, R.A. Clark, M.B. Kahn, and G. Williams. Lower limb angular velocity during walking at various speeds. *Gait & posture*, 65:190–196, 2018.

[22] M.J. Mueller, S.D. Minor, S.A. Sahrmann, J.A. Schaaf, and M.J. Strube. Differences in the gait characteristics of patients with diabetes and peripheral neuropathy compared with age-matched controls. *Physical therapy*, 74(4):299–308, 1994.

[23] A. Mündermann, L. Mündermann, and T.P. Andriacchi. Amplitude and phasing of trunk motion is critical for the efficacy of gait training aimed at reducing ambulatory loads at the knee. *Journal of biomechanical engineering*, 134(1), 2012.

[24] S. Nadeau, D. Gravel, A.B. Arsenault, and D. Bourbonnais. Plantarflexor weakness as a limiting factor of gait speed in stroke subjects and the compensating role of hip flexors. *Clinical Biomechanics*, 14(2):125–135, 1999.

[25] M.G. Pandy, Y. Lin, and H.J. Kim. Muscle coordination of mediolateral balance in normal walking. *Journal of biomechanics*, 43(11):2055–2064, 2010.

[26] O. Pinzone, M.H. Schwartz, and R. Baker. Comprehensive non-dimensional normalization of gait data. *Gait & posture*, 44:68–73, 2016.

[27] A. Rajagopal, C.L. Dembia, M.S. DeMers, D.D. Delp, J.L. Hicks, and S.L. Delp. Full-body musculoskeletal model for muscle-driven simulation of human gait. *IEEE transactions on biomedical engineering*, 63(10):2068–2079, 2016.

[28] J.A. Reinbolt, A. Seth, and S.L. Delp. Simulation of human movement: applications using opensim. *Procedia Iutam*, 2:186–198, 2011.

[29] R. Rethwilm, H. Böhm, C. U Dussa, and P. Federolf. Excessive lateral trunk lean in patients with cerebral palsy: is it based on a kinematic compensatory mechanism? *Frontiers in Bioengineering and Biotechnology*, 7, 2019.

[30] J. Riad, Y. Haglund-Akerlind, and F. Miller. Power generation in children with spastic hemiplegic cerebral palsy. *Gait & posture*, 27(4):641–647, 2008.

[31] S.A. Roelker, E.J. Caruthers, R.K. Baker, N.C. Pelz, A.M.W. Chaudhari, and R.A. Siston. Interpreting musculoskeletal models and dynamic simulations: causes and effects of differences between models/. *Annals of biomedical engineering*, 45(11):2635–2647, 2017.

[32] J. Romkes and R. Brunner. An electromyographic analysis of obligatory (hemiplegic cerebral palsy) and voluntary (normal) unilateral toe-walking. *Gait & posture*, 26(4):577–586, 2007.

[33] F. Salami, M. Niklasch, B.K. Krautwurst, T. Dreher, and S.I. Wolf. What is the price for the duchenne gait pattern in patients with cerebral palsy? *Gait & posture*, 58:453–456, 2017.

[34] S. Schmid, K. Schweizer, J. Romkes, S. Lorenzetti, and R. Brunner. Secondary gait deviations in patients with and without neurological involvement: a systematic review. *Gait & posture*, 37(4):480–493, 2013.

[35] O. Sofuwa, A. Nieuwboer, K. Desloovere, A. Willems, F. Chavret, and I. Jonkers. Quantitative gait analysis in parkinson's disease: comparison with a healthy control group. *Archives of physical medicine and rehabilitation*, 86(5):1007–1013, 2005.

[36] G. Sutton. Hamstrung by hamstring strains: a review of the literature. *Journal of Orthopaedic & Sports Physical Therapy*, 5(4):184–195, 1984.

[37] Z. Svoboda, L. Bizovska, M. Janura, E. Kubonova, K. Janurova, and N. Vuillerme. Variability of spatial temporal gait parameters and center of pressure displacements during gait in elderly fallers and nonfallers: A 6-month prospective study. *PloS one*, 12(2):e0171997, 2017.

[38] E. van der Kruk, F.C.T. van der Helm, H.E.J. Veeger, and A.L. Schwab. Power in sports: A literature review on the application, assumptions, and terminology of mechanical power in sport research. *Journal of biomechanics*, 79:1–14, 2018.

[39] J. van der Ploeg. The impact of medio-lateral trunk movement on mechanical energy generation and distribution during gait. 2019.

[40] K. Veerkamp, W. Schallig, J. Harlaar, C. Pizzolato, C.P. Carty, D.G. Lloyd, and M.M. van der Krogt. The effects of electromyography-assisted modelling in estimating musculotendon forces during gait in children with cerebral palsy. *Journal of biomechanics*, 92:45–53, 2019.

[41] L. Vossen. The relation between medio-lateral trunk movements and ankle power and work during the push off phase of gait. 2019.

[42] N.F.J. Waterval, M. Brehm, H.E. Ploeger, F. Nollet, and J. Harlaar. Compensations in lower limb joint work during walking in response to unilateral calf muscle weakness. *Gait & posture*, 66:38–44, 2018.

[43] D.A. Winter. Biomechanical motor patterns in normal walking. *Journal of motor behavior*, 15(4):302–330, 1983.

[44] D.A. Winter. Energy generation and absorption at the ankle and knee during fast, natural, and slow cadences. *Clinical orthopaedics and related research*, (175):147–154, 1983.

[45] F.E. Zajac and M.E. Gordon. Determining muscle's force and action in multi-articular movement. *Exercise and sport sciences reviews*, 17(1):187–230, 1989.

[46] J.A. Zeni Jr, J.G. Richards, and J.S. Higginson. Two simple methods for determining gait events during treadmill and overground walking using kinematic data. *Gait & posture*, 27(4):710–714, 2008.

Appendix A

Markers

Table A.1: Marker list. *List of all the markers that are used for motion tracking, extracted from the thesis of Vossen [41].*

Segment	Marker	Abbreviation	Anatomical/ Tracking
Calcaneus	Fifth metatarsal distal	M5D*	Anatomical + Tracking
	First metatarsal distal	M1D*	Anatomical + Tracking
	Calcaneus	CAL*	Anatomical + Tracking
	Second metatarsal base	M2B*	Tracking
	Sustentaculum tali	STL*	Tracking
Tibia	Lateral malleolus	LMAL*	Anatomical + Tracking
	Medial malleolus	MMAL*	Anatomical
	Head of fibula	HFIB*	Tracking
	Tibial tuberosity	TTUB*	Tracking
	Shank shin	SSH*	Tracking
Femur	Lateral epicondyle femur	FLE*	Anatomical + Tracking
	Medial epicondyle femur	FME*	Anatomical
	Thigh anterior proximal	TAP*	Tracking
	Thigh anterior distal	TAD*	Tracking
	Thigh lateral	TL*	Tracking
	Thigh posterior proximal	TPP*	Tracking
	Thigh posterior distal	TPD*	Tracking
Pelvis	Anterior superior iliac spine	ASIS*	Anatomical + Tracking
	Posterior superior iliac spine	PSIS*	Anatomical + Tracking
Torso	Tenth thoracic vertebrae	T10	Anatomical + Tracking
	Second thoracic vertebrae	T2	Anatomical + Tracking
	Incisura jugularis	IJ	Anatomical + Tracking
	Sternal angle	SA	Anatomical + Tracking
	Neck	IN	Anatomical + Tracking
	Cheek bone	CB*	Anatomical + Tracking
	Acromion	ACR*	Anatomical + Tracking
Humerus	Lateral epicondyle humerus	HLE*	Anatomical + Tracking
	Medial epicondyle humerus	HME*	Anatomical + Tracking
Radius	Wrist	USP*	Anatomical + Tracking

* = Marker has a left and a right version.

Appendix B

Subject characteristics

Table B.1: Subject characteristics. *Extracted from the thesis of Vossen [41].*

Subject	Gender (male/ female)	Age (years)	Length (cm)	Weight (kg)
1	M	23.8	192.2	81.9
2	F	24.3	168.9	67.7
3	F	33.8	177.5	76.3
4	F	25.2	163.4	58.4
5	M	20.7	177.8	67.8
6	F	25.1	174.0	74.9
7	F	49.9	164.4	59.7
8	M	23.6	180.4	76.3
9	M	25.5	170.4	56.8
10	M	25.3	178.7	84.7

Appendix C

Muscle abbreviations

Table C.1: Muscle abbreviations. *Each muscle and linear actuator have a left and a right version except for the linear actuators at the lumbar joint [27].*

Muscle	Abbreviation
Adductor brevis	addbrev
Adductor longus	addlong
Adductor magnus distal part	addmagDist
Adductor magnus ischial part	addmagIsch
Adductor magnus middle part	addmagMid
Adductor magnus proximal part	addmagProx
Biceps femoris long head	bflh
Biceps femoris short head	bfsh
Extensor digitorum longus	edl
Extensor hallucis longus	ehl
Flexor digitorum longus	fdl
Flexor hallucis longus	fhl
Gastrocnemius lateral head	gaslat
Gastrocnemius medial head	gasmed
Gluteus maximus superior part	glmax1
Gluteus maximus middle part	glmax2
Gluteus maximus inferior part	glmax3
Gluteus medius anterior part	glmed1
Gluteus medius middle part	glmed2
Gluteus medius posterior part	glmed3
Gluteus minimus anterior part	glmin1
Gluteus minimus middle part	glmin2
Gluteus minimus posterior part	glmin3
Gracilis	grac
Iliacus	iliacus
Peroneus brevis	perbrev
Peroneus longus	perlong
Piriformis	piri
Psoas	psoas
Rectus femoris	recfem
Sartorius	sart
Semimembranosus	semimem
Semitendinosus	semiten
Soleus	soleus
Tensor fascia latae	tfl
Tibialis anterior	tibant
Tibialis posterior	tibpost
Vastus intermedius	vasint

Muscle abbreviations (continued)

Muscle	Abbreviation
Vastus lateralis	vaslat
Vastus medialis	vasmed
Linear actuator at the lumbar extension joint	lumbar ext
Linear actuator at the lumbar bending joint	lumbar bend
Linear actuator at the lumbar rotation	lumbar rot
Linear actuator at the shoulder flexion joint	shoulder flex
Linear actuator at the shoulder adduction joint	shoulder add
Linear actuator at the shoulder rotation joint	shoulder rot
Linear actuator at the elbow flexion joint	elbow flex
Linear actuator at the pro-/ supination joint	pro sup
Linear actuator at the wrist flexion joint	wrist flex
Linear actuator at the wrist deviation joint	wrist dev

Appendix D

Comparison literature

D.1 Kinematics

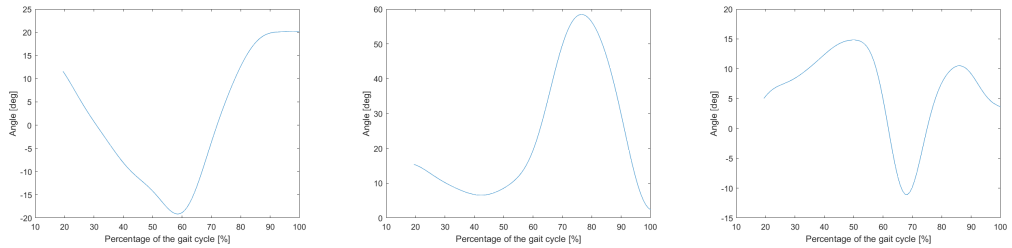

(a) Hip flexion angle current study (b) Knee flexion angle current study (c) Ankle dorsiflexion angle current study

Figure D.1: Joint angles current study normal walking condition

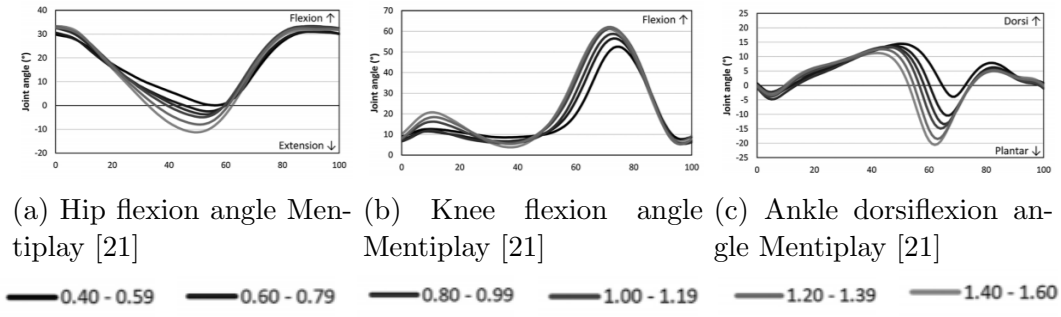

(a) Hip flexion angle Mentiplay [21] (b) Knee flexion angle Mentiplay [21] (c) Ankle dorsiflexion angle Mentiplay [21]

Figure D.2: Joint angles Mentiplay [21]

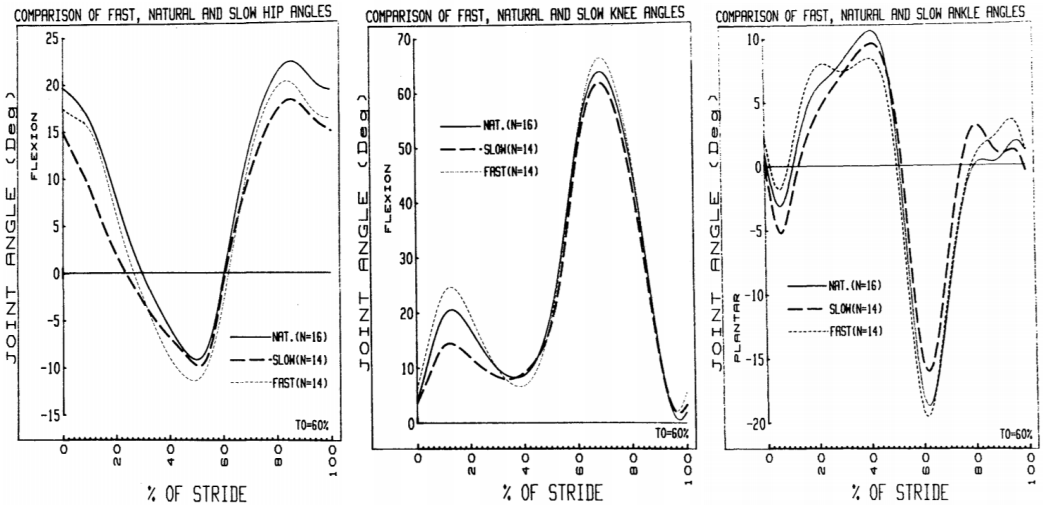

(a) Hip flexion angle Winter [43] (b) Knee flexion angle Winter [43] (c) Ankle dorsiflexion angle Winter [43]

Figure D.3: Joint angles Winter [43]

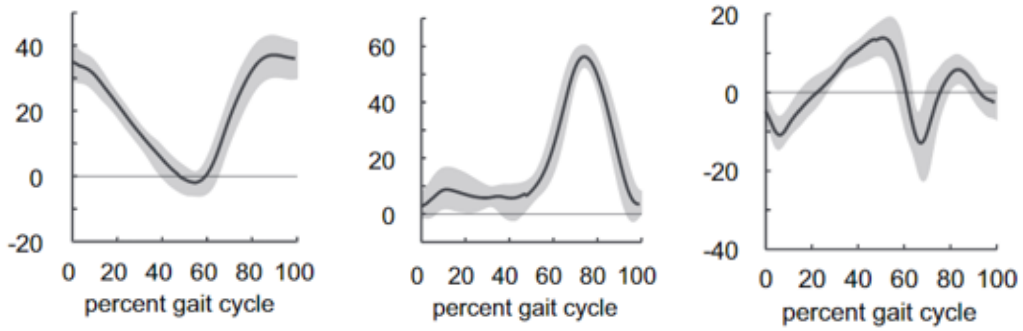

(a) Hip flexion angle Liu [18] (b) Knee flexion angle Liu [18] (c) Ankle dorsiflexion angle Liu [18]

Figure D.4: Joint angles Liu [18]

D.2 Kinetics

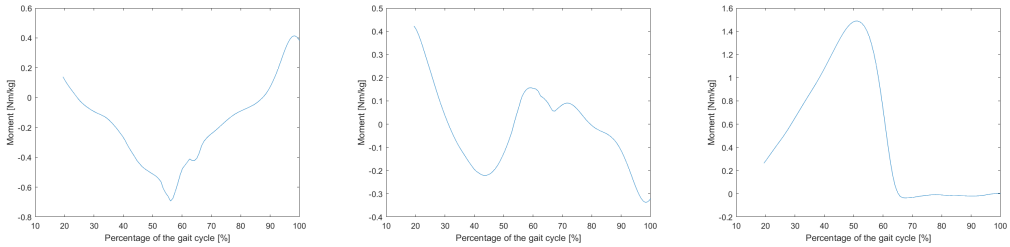

(a) Hip extension moment current study (b) Knee extension moment current study (c) Ankle plantar flexion moment current study

Figure D.5: Joint moments current study normal walking condition

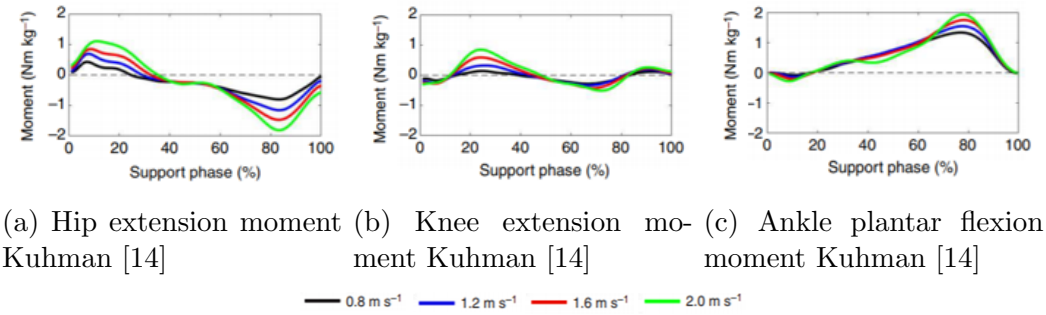

(a) Hip extension moment Kuhman [14] (b) Knee extension moment Kuhman [14] (c) Ankle plantar flexion moment Kuhman [14]

Figure D.6: Joint moments Kuhman [14]

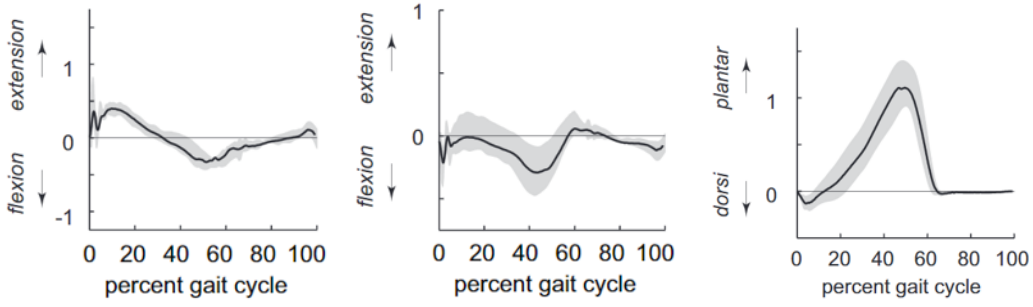

(a) Hip extension moment Liu [18] (b) Knee extension moment Liu [18] (c) Ankle plantar flexion moment Liu [18]

Figure D.7: Joint moments Liu [18]

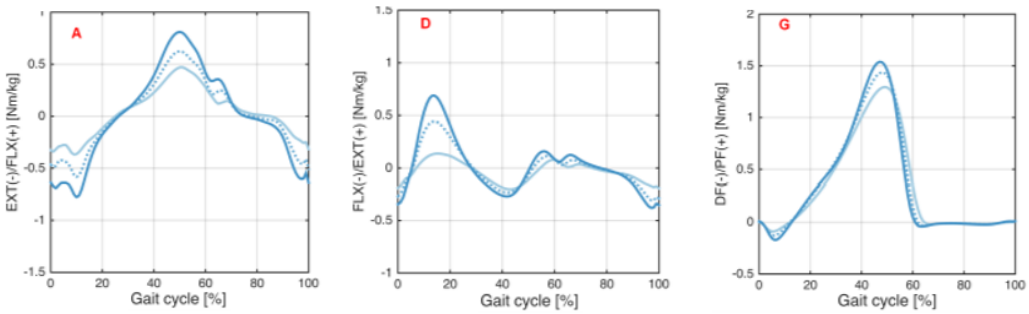

(a) Hip flexion moment Fukuchi [5]

(b) Knee extension moment Fukuchi [5]

(c) Ankle plantar flexion moment Fukuchi [5]

Figure D.8: Joint moments Fukuchi [5]